J. Fluid Mech. (1992), *vol.* 240, *pp.* 1–30
Printed in Great Britain

Instability of bounded flows with elliptical streamlines

By E. B. GLEDZER AND V. M. PONOMAREV
Institute of Atmospheric Physics, Russian Academy of Sciences, Moscow, 109017, Russia

(Received 2 May 1990 and in revised form 16 December 1991)

In connection with the recent investigations of the instability of unbounded elliptical flows, some methods are discussed for the study of the instability of bounded flows. The stability of a 'basic flow' which is two-dimensional and rotating, with elliptical streamlines similar to the elliptical section of an experimentally studied cavity, is investigated in the framework of linear theory (for circular rotation, the flow discussed is stable). The regions of instability for three-dimensional disturbances are found in the plane of the parameters defining the geometry of the system (the height of the ellipsoidal cavity and the degree of ellipticity). It is shown that two types of instability exist, characterized by either monotone or oscillatory growth of the amplitudes of small disturbances.

The influence of the Coriolis force field on this instability mechanism is also studied. Rotation of the system as a whole changes the regions of instability in parameter space characterizing the geometry of the cavity and the wavenumbers of unstable disturbances. As a result, the Coriolis force may stabilize or destabilize the basic flow for a given geometry.

The instability of rotating density-stratified flow with elliptical streamlines is also considered.

1. Introduction

The recent investigations of the three-dimensional elliptical instability in an infinite space performed by Pierrehumbert (1986), Bayly (1986), Landman & Saffman (1987), Waleffe (1990) have shown the necessity of the further development of theoretical and experimental studies of this type of instability for bounded flows. The theoretical solution for unbounded elliptical rotation presented in the above papers describes the development of spatially periodic disturbances of planar form superimposed on a basic two-dimensional elliptical eddy with spatially uniform vorticity. For this solution the nonlinear terms of the hydrodynamic equations are equal to zero identically. A more general case of this type of disturbance superimposed on a basic flow with uniform rates of strain was considered by Craik & Criminale (1986) (see also Craik 1988, 1989). The stability theory of unbounded elliptical rotation does not determine the lengthscale of unstable disturbances and the structures of instabilities are independent of it.

The existence of the exact solution for wavelike disturbances is connected with unboundedness of the flow. But the boundedness of the liquid volume is an essential condition for experimental investigation of the elliptical instability. Since streamlines of the basic flow are elliptical, it is natural to investigate this type of instability using elliptical containers (a cylinder or a three-axis ellipsoid).

The instability of elliptical rotation resulting in disturbances with spatially non-uniform vorticity was originally described by Gledzer *et al.* (1974) for a three-axis ellipsoid with a particular ratio of the axis. The experiments on ellipsoids were performed with the objective of studying flows with velocity components that depend linearly on the coordinates (Obukhov & Dolzhansky 1975). Classic results of Greenhill (1879), Hough (1895) and Poincaré (1910) predict the known condition that there is stability for rotation of fluid around the short and long axes of an ellipsoid and instability for rotation around the middle axis. The experiments mentioned above have confirmed the theory for the short and middle axes, but at the same time have shown some unexpected results for elliptical rotation around the long axis: for some values of the axes ratio it turned out to be unstable. A two-eddy pattern of motion was observed only for a certain interval of the long-axis length (see also Roesner & Schmieg 1980). The development of disturbances in this case has been investigated theoretically by expanding the velocity fields in terms of polynomials in the spatial coordinates (Gledzer & Ponomarev 1977*a*).

Some theoretical approaches to the stability of liquid motion in an elliptical cylinder together with an experimental study were presented by Gledzer *et al.* (1975). The experiments for elliptical cylinders were connected with an investigation of elliptical instability as one of the mechanisms for the generation of vortex structures on a background of velocity fields with similar to elliptical streamlines. The possible role of this type of instability was hypothesized, together with a cascade process of energy transfer for shear-flow turbulence. A related problem was discussed by Orszag & Patera (1983), Herbert (1983), Pierrehumbert & Widnall (1982) and Bayly, Orszag & Herbert (1988) concerning the secondary instability of shear flows.

The experiments on both elliptical cylinders and ellipsoids have demonstrated a qualitative difference in the behaviour of the disturbances with small changes of the container length. In the first case, a slow decay of the main elliptical rotation was observed, probably with small-scale instabilities. In the other case, the generation of secondary vortex structures occurs with considerable inclination of their axis rotation to the axis of the cylinder.

Such experiments made it possible to isolate the effects of the elliptical instability since the influence on the other instabilities of neighbouring container parameters looks almost identical. Experiments on elliptical cylinders with variable eccentricity were performed by Chernous'ko (1978) to separate the influence of the different types of instabilities from the large-scale elliptical one. For this case small changes of eccentricity produce transitions between stable and unstable elliptical rotation around the main axis of the cylinder.

The experiments described in this paper were carried out on containers with walls at rest. Malkus (1989) has performed an experiment to detect elliptical instability in a flow generated by rotation of the walls of an elastic elliptical cylinder (see also Malkus & Waleffe 1991), which reduces the effects of small-scale instabilities in the sidewall boundary layer.

The stability of an elliptical filament in an unbounded velocity field with a uniform rate of strain is intermediate between that of unbounded and bounded elliptical instability. It was considered by Tsai & Widnall (1976) using resonant theory, in a different formulation by Vladimirov, Ribak & Tarasov (1983*a*) and Vladimirov & Ilyjn (1988) and for finite values of eccentricity by Robinson & Saffman (1984).

The important feature of bounded elliptical instability is the existence of the horizontal scale (the mean width of the vessels or filament). Hence the investigation

of bounded elliptical flows allows us to find the relationship between the parameters of the main unstable disturbances and the horizontal scale of the elliptical rotation.

The aim of this paper is twofold. First, it is to describe the instabilities of bounded elliptical flows and the relation with the unbounded case. Second, it is to connect the analysis for elliptical cylinders where the Galerkin approximations are used, and for ellipsoids where it is possible to find exact solutions of a linear problem.

The paper is organized as follows. In §2 a general formulation of the liquid rotation stability problem in a cavity with elliptical sections is made. The Galerkin method is used in the framework of a linear theory on the basis of the eigenfunctions for the circular liquid rotation problem. In §3 the method is illustrated for an elliptical cylinder (and at the beginning of §4 for a three-axis ellipsoid). The main types of instability are determined in terms of the character of disturbance growth. A comparison of the results following from stability theory for bounded and unbounded flows is made. In §3.2 we give a brief summary of experiments and their comparison with the theory. In §4 a method of instability study for an ellipsoid based on a polynomial representation in the coordinates of the velocity field is presented. Thus an exact solution for the linear instability problem is obtained. A comparison with the experiments for various ellipsoids is made and a simple model for nonlinear interaction of the main elliptical rotation and unstable disturbances is also suggested. The model provides a description of the experimentally observed phenomenon of the transition from one steady state of the hydrodynamical system to another. In §5 we consider the influence of the Coriolis force field on the development of elliptical instability both in the elliptical cylinder and the three-axis ellipsoid. For unbounded elliptical rotation the effect of fluid stratification is studied.

The results concerning the stability of a stratified elliptical eddy and the influence of the Coriolis force field are likely to be of geophysical interest.

2. General formulation

2.1. *Statement of the problem*

The velocity field with elliptical streamlines

$$\boldsymbol{u}_0(x,y) = \Omega\left(-\frac{a}{b}y\boldsymbol{i}+\frac{b}{a}x\boldsymbol{j}\right), \quad p_0 = \tfrac{1}{2}\rho\Omega^2(x^2+y^2) \tag{2.1}$$

(where $\boldsymbol{i},\boldsymbol{j},\boldsymbol{k}$ are unit vectors corresponding to coordinates x,y,z; $\Omega = \text{const.}$) is a stationary solution of the equations of an incompressible ideal fluid for an unbounded domain or a volume having the surface

$$(x/a)^2+(y/b)^2 = f^2(z/L), \tag{2.2}$$

where f is an arbitrary function.

The vorticity $\boldsymbol{\Omega}_a$ of this flow is spatially constant, $\boldsymbol{\Omega}_a = (a^2+b^2)/(ab)\,\Omega\boldsymbol{k}$.

The linear stability of the elliptical flow (2.1) to small inviscid perturbations $\boldsymbol{u} = (u,v,w)$, p is governed by the equations (density $\rho = 1$)

$$\frac{\partial \boldsymbol{u}}{\partial t}+\boldsymbol{u}_0\cdot\nabla\boldsymbol{u}+\boldsymbol{u}\cdot\nabla\boldsymbol{u}_0 = -\nabla p, \quad \nabla\cdot\boldsymbol{u} = 0. \tag{2.3}$$

In new variables $\boldsymbol{u}', p'$,

$$\left.\begin{gathered} x' = \frac{x}{a}, \quad y' = \frac{y}{b}, \quad z' = \frac{z}{R}, \quad u' = \frac{u}{a}, \quad v' = \frac{v}{b}, \quad w' = \frac{w}{R}, \quad t' = \Omega t, \\ R = \left(\frac{a^2+b^2}{2}\right)^{\frac{1}{2}}, \quad p' = \frac{p}{\Omega^2R^2}, \end{gathered}\right\} \tag{2.4}$$

equations (2.3) take the form (we shall henceforth omit the primes)

$$\mathrm{D}u - v = -\frac{1}{1+\epsilon}\frac{\partial p}{\partial x}, \quad \mathrm{D}v + u = -\frac{1}{1-\epsilon}\frac{\partial p}{\partial y}, \tag{2.5}$$

$$\mathrm{D}w = -\frac{\partial p}{\partial z}, \quad \nabla\cdot\boldsymbol{u} = 0, \quad \mathrm{D} = \frac{\partial}{\partial t} + x\frac{\partial}{\partial y} - y\frac{\partial}{\partial x}, \quad \epsilon = \frac{a^2-b^2}{a^2+b^2}, \tag{2.6}$$

with the boundary condition $u_n = 0$. Parameter ϵ characterizes the degree of ellipticity of the flow streamlines.

A single equation for the velocity w directed along the z-axis can be obtained from (2.5) and (2.6) (Gledzer, Dolzhansky & Obukhov 1981, and, in another form, Waleffe 1990):

$$\left.\begin{aligned} \left[\mathrm{D}^2\nabla_\epsilon^2 + 4(1-\epsilon^2)\frac{\partial^2}{\partial z^2}\right] w &= \epsilon(4+\mathrm{D}^2)\left(\frac{\partial^2}{\partial x^2} - \frac{\partial^2}{\partial y^2}\right) w, \\ \nabla_\epsilon^2 &= \frac{\partial^2}{\partial x^2} + \frac{\partial^2}{\partial y^2} + (1-\epsilon^2)\frac{\partial^2}{\partial z^2}, \end{aligned}\right\} \tag{2.7}$$

which is convenient to use for a flow in a cylindrical or an unbounded domain.

The solution of (2.3) described by Bayly (1986) (see also Craik & Criminale 1986) has the form

$$\boldsymbol{u} = \mathrm{Re}\,(\hat{\boldsymbol{u}}(t)\,\mathrm{e}^{k(t)\cdot r}), \quad \boldsymbol{k}\cdot\hat{\boldsymbol{u}} = 0. \tag{2.8}$$

The nonlinear terms in (2.8) vanish identically by virtue of the continuity equation, so $\boldsymbol{u}$ is the nonlinear solution for unbounded flow. It may be exponentially growing for certain correlations between k_z^2 and $k_x^2 + k_y^2$. The Fourier modes (2.8) can be superposed to construct various solutions (Bayly 1986; Waleffe 1990).

We shall use the Galerkin method originating from the vector form of the system (2.5), (2.6). The Galerkin method for vector equations may be more convenient for bounded domains and give the possibility of constructing the dynamical system describing the nonlinear processes (see §4.4).

2.2 *Galerkin method: eigenfunctions of 'solid-body' rotation*

In the cylindrical coordinate system for the 'deformed' variables introduced, (2.5), (2.6) take the form (for these variables initial elliptical streamlines correspond to circular streamlines)

$$\boldsymbol{M}\left(\frac{\partial \boldsymbol{u}}{\partial t} + \boldsymbol{H}\boldsymbol{u}\right) = -\nabla p, \quad \nabla\cdot\boldsymbol{u} = 0, \tag{2.9a}$$

$$\boldsymbol{M} = \boldsymbol{I} + \epsilon\boldsymbol{T}, \quad \boldsymbol{H} = \boldsymbol{I}\frac{\partial}{\partial\varphi} + 2\boldsymbol{\Lambda}, \tag{2.9b}$$

$$\boldsymbol{\Lambda} = \begin{vmatrix} 0 & -1 & 0 \\ 1 & 0 & 0 \\ 0 & 0 & 0 \end{vmatrix}, \quad \boldsymbol{T} = \begin{vmatrix} \cos 2\varphi & -\sin 2\varphi & 0 \\ -\sin 2\varphi & -\cos 2\varphi & 0 \\ 0 & 0 & 0 \end{vmatrix}, \tag{2.9c}$$

where $\boldsymbol{I}$ is a unit matrix. The system (2.9*a–c*) is considered in the region

$$0 \leqslant r < f(zR/L), \quad 0 \leqslant \varphi < 2\pi, \quad 0 < z < L/R, \tag{2.10}$$

with the boundary condition $u_n = 0$.

We shall seek a solution of (2.9) in the form

$$\boldsymbol{u} = \sum_{\alpha} C_{\alpha} \exp(\mathrm{i}st)\, \boldsymbol{u}_{\alpha}, \tag{2.11}$$

where $\boldsymbol{u}_{\alpha}$ is the solution of the eigenvalue problem for unperturbed equations ($\epsilon = 0$)

$$\boldsymbol{H}\boldsymbol{u}_{\alpha} + \nabla p_{\alpha} = -\mathrm{i}\omega \boldsymbol{u}_{\alpha}, \quad \nabla \cdot \boldsymbol{u}_{\alpha} = 0, \tag{2.12}$$

with the same condition $u_n = 0$ on the surface of the volume. This solution describes the inertial waves in a fluid rotating as a whole (Greenspan 1968). Experiments by McEwan (1970) have shown that such solutions give a very accurate description of individual modes in a rotating cylinder containing viscous fluid at sufficiently high Reynolds numbers.

The operator $\mathrm{i}\boldsymbol{H}$ is self-adjoint, with the scalar product being determined by

$$(\boldsymbol{u}, \boldsymbol{v}) = \int_{V} \boldsymbol{u} \cdot \boldsymbol{v}^{*} r \, \mathrm{d}r \, \mathrm{d}\varphi \, \mathrm{d}z, \tag{2.13}$$

where the integration is extended over the region occupied by the fluid, hence the characteristic values ω in (2.12) are real. Physically that means that the 'solid-body' rotation of fluid is stable. The functions $\boldsymbol{u}_{\alpha}$ at various eigenvalues are orthogonal in the sense of (2.13).

They are expressed through $p_{\alpha}(r, z)$ by the relations

$$\left.\begin{aligned} u_{r\alpha} &= -\frac{\mathrm{i}}{4-q_{\alpha}^2}\left(q_{\alpha}\frac{\partial p_{\alpha}}{\partial r} + \frac{2n}{r}p_{\alpha}\right)\exp(\mathrm{i}n\varphi), \\ u_{\varphi\alpha} &= \frac{1}{4-q_{\alpha}^2}\left(2\frac{\partial p_{\alpha}}{\partial r} + \frac{q_{\alpha} n}{r}p_{\alpha}\right)\exp(\mathrm{i}n\varphi), \\ w_{\alpha} &= \frac{\mathrm{i}}{q_{\alpha}}\frac{\partial p_{\alpha}}{\partial z}\exp(\mathrm{i}n\varphi), \quad q_{\alpha} = \omega_{\alpha} + n, \quad n = 0, \pm 1, \pm 2, \ldots. \end{aligned}\right\} \tag{2.14}$$

The function p_{α} satisfies the equation

$$\frac{1}{r}\frac{\partial}{\partial r} r \frac{\partial p_{\alpha}}{\partial r} - \frac{n^2}{r^2} p_{\alpha} - \frac{4-q_{\alpha}^2}{q_{\alpha}^2}\frac{\partial^2 p_{\alpha}}{\partial z^2} = 0. \tag{2.15}$$

In the 'vector' subscript $\alpha = \{n, l\}$, the integer l numbers the eigenfunctions of (2.14), (2.15) for each given value n. The existence of solutions of (2.15) satisfying the boundary condition $u_n = 0$ leads to the restriction $|q_{\alpha}| \leqslant 2$.

Substituting (2.11) in (2.9*a*) (the continuity equation and the boundary conditions are satisfied automatically) and performing scalar multiplication of this equation by $\boldsymbol{u}_{\alpha}$, we obtain the system

$$\left.\begin{aligned} (s-\omega_{\alpha})\, C_{\alpha} N_{\alpha}^2 + \epsilon(s+n) \sum_{\beta} V_{\alpha\beta} C_{\beta} = 0, \\ N_{\alpha}^2 = (\boldsymbol{u}_{\alpha}, \boldsymbol{u}_{\alpha}), \quad V_{\alpha\beta} = (T\boldsymbol{u}_{\beta}, \boldsymbol{u}_{\alpha}), \\ \alpha = (n, l), \quad \beta = (n', l'). \end{aligned}\right\} \tag{2.16}$$

We use the formula $2\boldsymbol{T}\boldsymbol{\Lambda} = \partial \boldsymbol{T}/\partial\varphi$, which may be obtained from (2.9). The interaction coefficients $V_{\alpha\beta}$ satisfy the condition

$$V_{\alpha\beta} = V^*_{\beta\alpha} \tag{2.17}$$

and differ from zero only for eigenfunctions with wavenumbers n and $n\pm 2$. So (2.16) consists of two independent systems for odd and even values n. Notice also, that (2.16) is a generalized eigenvalue problem for s. The transformation to the conventional form may be done by reversing of the operator $(N^2_\alpha \delta_{\alpha\beta} + \epsilon V_{\alpha\beta})$ in (2.16).

Application of perturbation theory with the parameter ϵ to (2.16) shows that corrections to ω_{nl} have an imaginary part of first order in ϵ only if $\omega_{nl} = \omega_{n+2,l}$ or $\omega_* = \omega_{nl} = \omega_{n-2,l'}$. For example, in the latter case we have $q_{nl} > 0$ and $q_{n-2,l'} = q_{nl} - 2 < 0$, and the correction for a degenerate eigenvalue ω_* is

$$s - \omega_* = \pm \mathrm{i}\epsilon \frac{|V_{nl;n-2,l'}|}{N_{nl} N_{n-2,l'}} (q_{nl}(2-q_{nl}))^{\frac{1}{2}}. \tag{2.18}$$

Another variant of the perturbation theory for the problem (2.9) was presented by Vladimirov *et al.* (1983, 1988). We confine ourselves to the Galerkin approximations taking into account only large-scale disturbances in (2.16), having in mind a comparison with the results of experiments.

3. Instability in an elliptical cylinder

3.1. *Two types of instability of elliptical rotation*

The boundary conditions for (2.15) in the case of an elliptical cylinder are

$$\partial p_\alpha/\partial z = 0 \quad (z = 0, L/R), \quad q_\alpha \partial p_\alpha/\partial r + 2np_\alpha = 0 \quad (r = 1).$$

The solution of (2.15) is

$$\left.\begin{aligned} p_\alpha &= -(4-q_\alpha^2) J_n(h_\alpha r)\cos(k_m z), \\ q_\alpha h_\alpha J'_n(h_\alpha) + 2nJ_n(h_\alpha) &= 0, \quad q_\alpha^2 = \frac{4k_m^2}{h_\alpha^2 + k_m^2}, \\ J'_n(h) &= \mathrm{d}J_n/\mathrm{d}h, \quad k_m = \pi m R/L, \quad \alpha = (n, m, j), \end{aligned}\right\} \tag{3.1}$$

where j numbers the roots of (3.1).

The calculation of the interaction coefficients and norms in (2.16) yields

$$\left.\begin{aligned} N^2_\alpha &= (2\pi L/R)\,[2h^2_\alpha + n(2n-q_\alpha)(4-q^2_\alpha)/q^2_\alpha] J^2_n(h_\alpha), \\ V_{\alpha\alpha'} &= \tfrac{1}{2}(\pi L/R)\, h_\alpha h_{\alpha'} \delta_{m,m'} [\delta_{n,n'+2}(2+q_\alpha)(2-q_{\alpha'}) B_- \\ &\quad + \delta_{n,n'-2}(2-q_\alpha)(2+q_{\alpha'}) B_+], \\ B_\pm &= \int_0^1 J_{n\pm1}(h_\alpha r) J_{n\pm1}(h_{\alpha'} r)\, r\,\mathrm{d}r, \quad \alpha' = (n', m', j'). \end{aligned}\right\} \tag{3.2}$$

The subsystems from (2.16) are independent for different values of m, and summation occurs only on subscripts n' and j'. At the first order of perturbation theory, for $\epsilon \ll 1$, instability is possible only for interacting modes with neighbouring

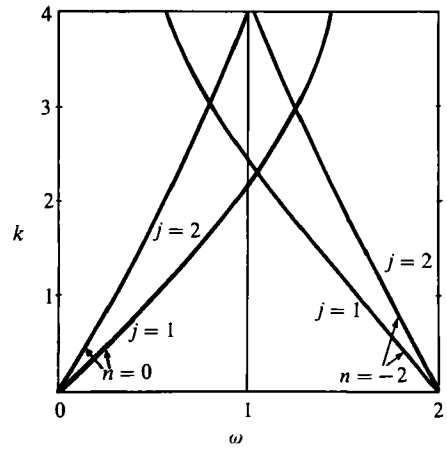

FIGURE 1. The dependence on k of the two first eigenvalues ω in (3.1) for the azimuthal wavenumbers $n = 0$ and $n = -2$.

frequencies. Let us consider the frequencies ω_α and $\omega_{\alpha'}$ so that $\omega_{\alpha'} \approx \omega_\alpha$ and $n' = n+2$ or $n' = n-2$. At first order, the systems (2.16) may be reduced to the form

$$\left.\begin{aligned}(s-\omega_a)\, C_\alpha N_\alpha^2 + \epsilon(s+n)\, V_{\alpha\alpha'} C_{\alpha'} = 0,\\ \epsilon(s+n')\, V_{\alpha'\alpha} C_\alpha + (s-\omega_{\alpha'})\, C_{\alpha'} N_{\alpha'}^2 = 0,\end{aligned}\right\} \tag{3.3}$$

which leads to the quadratic equation

$$(1-E^2)\, s^2 - [\omega_\alpha + \omega_{\alpha'} + E^2(n+n')]\, s + (\omega_\alpha \omega_{\alpha'} - E^2 n n') = 0, \tag{3.4}$$

$$E^2 = \epsilon^2 \frac{V_{\alpha\alpha'} V_{\alpha'\alpha}}{N_\alpha^2 N_{\alpha'}^2}.$$

The unstable disturbances have a growth rate σ and a frequency ω, $(s = \omega \pm i\sigma)$,

$$\left.\begin{aligned}\sigma^2 &= -\frac{[\omega_\alpha - \omega_{\alpha'} + E^2(n-n')]^2 + 4E^2 q_\alpha q_{\alpha'}}{4(1-E^2)^2},\\ \omega &= \frac{\omega_\alpha + \omega_{\alpha'} + E^2(n+n')}{2(1-E^2)}.\end{aligned}\right\} \tag{3.5}$$

The expression for the growth rate determines the regions of instability for the parameters $(L/R, \epsilon)$, where the flow is unstable with respect to disturbances with azimuthal wavenumber n and $n' = n+2$ with an accuracy of order ϵ^2.

So, for given cylinder geometry, the kind of unstable disturbance is connected with the distribution of natural frequencies (2.14) for a fluid rotating as a solid body (2.12): it follows from (3.5) that instability is possible only if $(\omega_\alpha - \omega_{\alpha'}) = O(E)$. The structure of this distribution is defined by (3.1).

The roots of (3.1) for given wavenumbers n, k and given the sign of q are placed between the roots of the equation $J_n(h') = 0$:

$$h'_{nj} \leqslant h_{nj} \leqslant h'_{n,j+1}. \tag{3.6}$$

The general character of the dependence of the first two eigenvalues $(j = 1, 2)$ on the wavenumber k for overlapping regions of the wavenumbers ω_{nj} for $n = 0$ and $n = -2$, is shown in figure 1 (compare Tsai & Widnall 1976). The points where the curves cross correspond to the corner points at $\epsilon = 0$ in the region of instability in the plane of parameter $\{L/R, \epsilon\}$ (figure 2*a*).

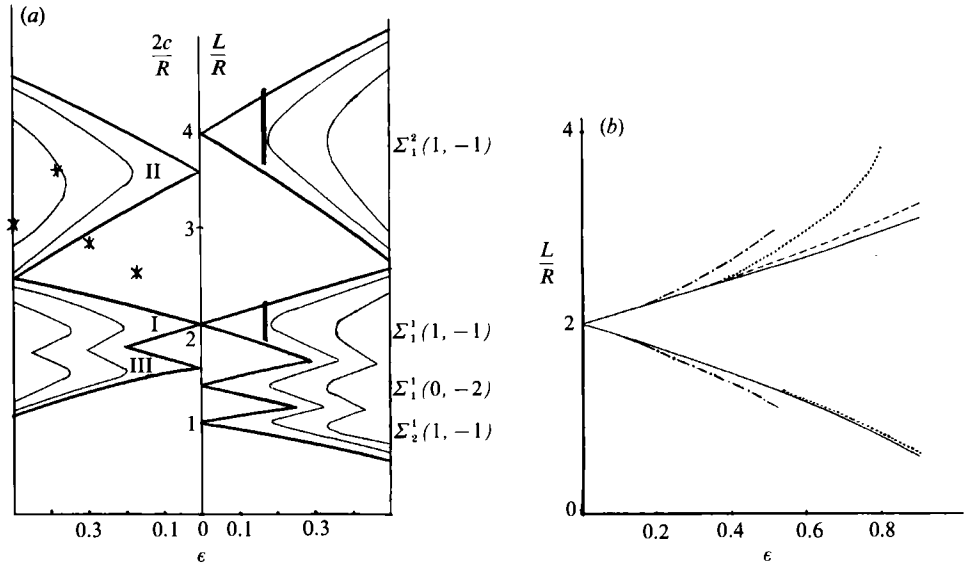

FIGURE 2. (*a*) The regions of large-scale elliptical instability in an elliptical cylinder (right) and a three-axis ellipsoid (left). $\Sigma_l^m(n,n')$ denote the types of unstable disturbances: n and n' are the azimuthal wavenumbers, m is the number of eddy structures on the z-axis, l is number of times the sign of the w-velocity changes on the r-axis. The thick vertical lines and stars indicate the intervals and values of parameters of corresponding experimentally investigated instabilities. The contours for each region are plotted in the interval 0.1 (in dimensionless variables (2.4)). (*b*) Comparison of the different approximations for the region $\Sigma_1^1(1,-1)$ of (*a*): ——, the approximation for (2.16) with $n, n' = \pm 1; j, j' = 1$; ----, the approximation for (2.16) with $n, n' = \pm 1, \pm 3, \pm 5; j, j' = 1$–$6$; ....., the approximation corresponding to Waleffe's solution; -·-·-, the Galerkin approximation for (2.7) with $n, n' = \pm 1$.

The condition of coincidence of the frequencies for wavenumbers n and $n-2$ is

$$\frac{2k}{(k^2+h_{nj}^2)^{\frac{1}{2}}}+\frac{2k}{(k^2+h_{n-2,j'}^2)^{\frac{1}{2}}}=2. \tag{3.7}$$

From (3.7) follows the inequality

$$k > \frac{h_{nj}h_{n-2,j'}}{h_{nj}+h_{n-2,j'}},$$

which shows that with increasing n the vertical size of unstable eddies decreases (from (3.6) it follows that $h_{nj} \to \infty$ for $n \to \infty$).

The wavenumbers $n = 1$, $n' = -1$ and $n = \pm 2$, $n' = 0$ yield the large-scale perturbations of the velocity field. In the first case, the frequency curves in figure 1 are symmetrical with respect to the line $\omega = 0$. Therefore, according to (3.5), instability with $\omega = 0$ to the first order in ϵ takes place as a result of the interaction of perturbation of equal scale. These regions of instability are defined by the corner points $L/R = \sqrt{3}\pi m/h_j$, where h_j are the roots of the equation $hJ_0(h)+J_1(h) = 0$. The values $L/Rm = 1.9898$ and 0.956 correspond to the two first roots of this equation.

Calculation of the growth rate according to (3.5) for the above sizes of cylinder gives (to first order in ϵ)

$$\sigma = \frac{9}{8}\frac{h_\alpha^2+1}{2h_\alpha^2+3}\epsilon, \tag{3.8}$$

which is identical to the result of Vladimirov, Ribak & Tarasov (1983*a*).

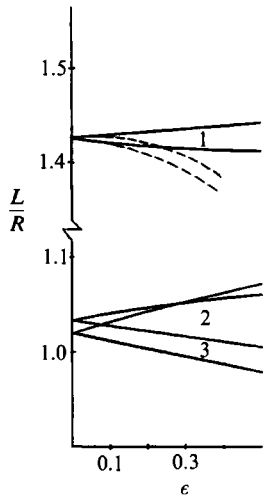

FIGURE 3. The regions of instability in an elliptical cylinder: the two-term approximation (3.3) for $\alpha = (-1, 1, 1)$, $\alpha' = (1, 1, 2)$ (curves 1); $\alpha = (0, 1, 1)$, $\alpha' = (2, 1, 2)$ (curves 2); $\alpha = (0, 1, 2)$, $\alpha' = (2, 1, 1)$ (curves 3). Dashed lines show the approximation for (2.16) with $n, n' = \pm 1, \pm 3, \pm 5$; $l, l' = 1$–6.

The corresponding instability regions for an elliptical cylinder are shown on the right-hand side of figure 2(*a*). They were calculated from (3.4) for $j = 1$, $m = 1, 2$ and $j = 2$, $m = 1$. The regions are denoted by the symbols Σ_l^m, where m indicates the periodicity of the perturbation on the z-axis, and l is the index of the root of equation (3.1). Therefore, $l-1$ is equal to the number of sign changes of the axial velocity w along the r-axis, and l can be regarded as a number of 'eddies' on the r-axis.

The region of large-scale instability for disturbances with even numbers $n = 0, \pm 2$ with corner point $L/R = 1.35$, is also presented in figure 2(*a*). The development of this instability is accompanied by oscillations with frequency of order of 1 (in non-dimensional variables). In the cases considered, instability is determined by interaction of eddies of similar scales. If these scales differ significantly, the width of the instability regions and growth rates are smaller by more than an order of magnitude than the region Σ_l^m. For illustration, such regions for $n = -1$, $n' = 1$ (curves 1); $n = 0$, $n' = 2$ (2, 3) and $j \neq j'$ are shown in figure 3.

Similar instability modes with odd values of n for an unbounded domain were found numerically by Pierrehumbert (1986) and analytically by Waleffe (1990). For the Waleffe solution, we must consider the modes with $h_\alpha \to \infty$ in (2.16). It follows then from (3.8) that the value of the growth rate for small ϵ, $\sigma = 9\epsilon/16$, does not depend on the perturbation scale.

The main difference between instabilities in bounded and unbounded flows is that the interaction between modes of various scales vanishes for the latter case, i.e.

$$\frac{V_{\alpha\alpha'} V_{\alpha'\alpha}}{N_\alpha^2 N_{\alpha'}^2} \to 0, \quad h_\alpha \to \infty, \quad h_{\alpha'} \to \infty, \quad (h_\alpha \neq h_{\alpha'}).$$

In this limit case the system (2.16) may be reduced to Waleffe's system describing the instability of the unbounded flow, with the help of the change $h_\alpha \to h$, $k^2 \to k^2(1-\epsilon^2)$, $C_{nm} \to (s+n) C_{nm}$. Hence, the oscillatory instability of unbounded flows within the framework of the model (3.3) may be connected only with the interaction of

the equal-scale modes in the radial direction (compare Waleffe 1990), where the disturbance scale h does not depend on the wavenumber n).

It may be noted that the boundaries of the instability region for $\epsilon \to 0$ give the same ratio $h^2/k^2 = 3$ for both bounded and unbounded flows. The values h and k are defined by the geometry of the cavity in which the elliptical rotation of fluid is unstable with respect to disturbances with wavenumbers $n = \pm 1$.

Of course the system (3.3) in which only the interaction between two modes is considered (the two-term Galerkin approximation) is the simplest and at first seems very rough for the description of the instability areas. A description of instability in the framework of the simplest systems is impossible for those areas L/R where the eigenvalue spectrum is very densely distributed. In this case the large-term approximation should be used. (For the instability in the Coriolis force field considered in §5 the coincidence and proximity of the eigenvalues ω_α can occur for several modes with different values of n, j.)

The validity of the two-term approximation was verified by considering the high-order terms in the decomposition (2.11). Approximations of the area $\Sigma_1^1(1, -1)$ are shown on figure 2(*b*) obtained with the above-mentioned terms $n, n' = \pm 1$; $j, j' = 1$ taken into account (solid lines) and from solving system (2.16) in which $n, n' = \pm 1$, ± 3, ± 5; $j, j' = 1$–6 (dashed line) (including the other additional terms does not alter this instability region in practice).

It follows from figure 2(*b*) that there is a variance between the two approximations only if $\epsilon > 0.5$, so that the areas shown in figure 2(*a*) describe the linear instability of the considered elliptical rotation sufficiently exactly.

The system (2.16) with $n, n'; j, j'$ as above reveals another instability region, including the dashed-line area in figure 3 that corresponds to the region 1. In this case the two-term approximation (3.3) with modes $n = -1$, $j = 1$; $n' = 1$, $j' = 2$ is valid only if $\epsilon < 0.1$.

The solution (2.11) may be represented as the superposition of the plane waves (2.8). In the variables (2.4) the wavevector $\boldsymbol{k}(t)$ has the form

$$\boldsymbol{k}(t) = (h\cos t, h\sin t, k), \tag{3.9}$$

and with the help of the known relation

$$J_n(hr) = \frac{(-\mathrm{i})^n}{2\pi}\int_0^{2\pi} \mathrm{e}^{-\mathrm{i}n\tau}\exp(\mathrm{i}hr\cos\tau)\,\mathrm{d}\tau,$$

we obtain the following expression for the w-velocity:

$$w(\boldsymbol{r}, t) = \mathrm{e}^{\mathrm{i}kz}\sum_\alpha C_\alpha(t)\,J_n(h_\alpha r)\,\mathrm{e}^{\mathrm{i}n\varphi} = \frac{1}{2\pi}\int_0^{2\pi}\sum_\alpha (-\mathrm{i})^n C_\alpha(t)\,\mathrm{e}^{\mathrm{i}n\pi}\exp[\mathrm{i}\boldsymbol{k}_\alpha(\tau)\cdot\boldsymbol{r}]\,d\tau. \tag{3.10}$$

For disturbances with the single scale $h_\alpha = h$, which correspond to the two-term Galerkin approximation with wavenumbers $n = \pm 1$ for the flow in a cylinder, (3.10) takes the form

$$w(\boldsymbol{r}, t) = \mathrm{e}^{\sigma t}\int_0^{2\pi} \hat{w}(t-\tau)\exp[\mathrm{i}\boldsymbol{k}(t-\tau)\cdot\boldsymbol{r}]\,\mathrm{d}\tau, \tag{3.11}$$

$$\hat{w}(t) = \frac{1}{2\pi}\sum_{n=\pm 1}(-\mathrm{i})^n C_n^0\,\mathrm{e}^{\mathrm{i}nt}, \quad (C_n(t) = \mathrm{e}^{\sigma t}C_n^0). \tag{3.12}$$

As shown by Waleffe (1990), (3.11) is also the solution for unbounded flow, if $\hat{w}(t)$ and σ are determined by an equation of Ince type originating from (2.7) and (3.9):

$$\left.\begin{aligned} &(1-a\cos 2t)\,\ddot{\hat{w}}+4a\sin 2t\dot{\hat{w}}+c\hat{w}=0,\\ &a=4\epsilon h^2/(h^2+k_\epsilon^2),\quad c=4k_\epsilon^2/(h^2+k_\epsilon^2). \end{aligned}\right\} \tag{3.13}$$

Then (3.12) is the first term in the perturbation theory for ϵ in (3.13). Accordingly the growth rate σ has an accuracy of order ϵ^2, which allows the possibility of using the unbounded flow theory connected with the representation (2.8) for the determination of the instability area $\Sigma(1,-1)$ in the cylinder.

For a comparison with the area $\Sigma_1^1(1,-1)$, the instability area for unbounded elliptical rotation following from Waleffe's solution for (3.9) is marked in figure 2(*b*) (points) (our parameters $k=k_1$ and $h=h_{1,1}$ in (3.1)–(3.8) are related with Waleffe's parameters μ and κ by $k=\mu$, $h=\kappa(1-\epsilon)^{\frac{1}{2}}$). It is significant that h is not arbitrary as for unbounded rotation, but is defined by (3.1).

The limits of the instability area $\Sigma_1^1(1,-1)$ obtained by the Galerkin method for (2.7), which is considered together with the boundary condition $u_n=0$ $(r=1)$, are also shown in figure 2(*b*) (dot–dash lines). Within the perturbations with wavenumbers $n=\pm 1$ we can obtain (Gledzer *et al.* 1980) the equation governing the area of instability mentioned:

$$\frac{\sqrt{3}\pi m}{h_-}(1-\tfrac{3}{4}\epsilon)<\frac{L}{R}<\frac{\sqrt{3}\pi m}{h_+}(1+\tfrac{3}{4}\epsilon),$$

$$3k^2=(1\pm\tfrac{3}{2}\epsilon)h_\pm^2,\quad h_\pm J_0(h_\pm)(1\pm\tfrac{3}{2}\epsilon)+J_1(h_\pm)=0.$$

Comparing the regions of the wavelike instability for disturbances with wavenumbers $n=\pm 1$ obtained by the methods mentioned above we find that consideration of the higher decomposition harmonics weakly changes the borders of the instability area, and the correlation between the vertical and horizontal scales h/k in it is rather well determined by the unbounded flow theory.

3.2. *Some experimental results on elliptical flow in a cylinder*

This account of the experiments and interpretation of their results as elliptical instability is from A. M. Obukhov.

The experiments were carried out by the following method. A transparent elliptical-shaped container with a liquid (salt water) was set in rotation, which continued for several minutes until the liquid and the container were moving as a single solid body, and then the container was brought suddenly to rest. The liquid continued to move by inertia with a spatially constant vorticity at the initial time.

The main semi-axes of the cylinder were 5 cm and 6 cm and the height could be varied from 8 cm to 37 cm. The rotation speed usually changed from 200 to 500 r.p.m. Visualization of the flow was achieved by markers, which were small balls with a density equal to the liquid density.

Contrary to the recent experiments by Malkus (1989) where the fluid motion was set up by rotating the walls of an elastic cylinder, in these experiments the boundary layer begins to form immediately after stopping. Additionally, two weak eddy flows are formed around the 'poles' arising from the Ekman boundary layers and corresponding circulation. However, this perturbation of the elliptical flow probably does not greatly influence the large-scale instability, because two distinct pictures of the secondary flows are observed for very similar heights of the cylinder.

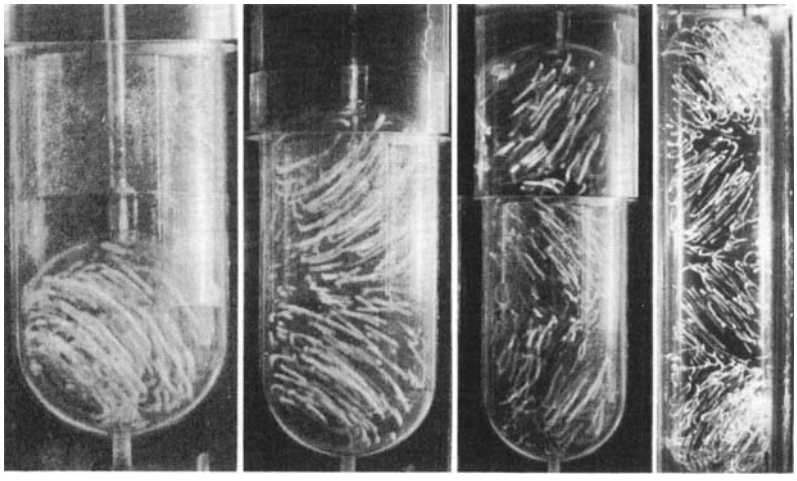

FIGURE 4. Photographs of eddy flows formed as a result of elliptical instability in an elliptical cylinder.

In the first case, if the sizes of the cylinder are within the stability regions, the rotation of fluid is slowly decaying over a few minutes. In the other case, we have a fast development of flow with vertical velocity.

Photographs of different vortex flows arising through the process of elliptical rotation hydrodynamic instability are shown in figure 4 (Chernous'ko 1978; Boubnov 1981). The range of variation of L/R (in figure $2a$, $\epsilon = 0.18$) for which disturbances (2.11) with $m = 1, 2$ were observed, are marked by thick vertical lines in figure $2(a)$. It is seen from comparison with the theoretical results, that for regions Σ_1^1 and Σ_1^2 there is agreement with the theory, although with increasing L/R there is a discrepancy relative to predicted intervals.

This effect is probably connected with the perturbations of elliptical flow arising after stopping of the cylinder. There are at least two types of perturbation. The first is the small-scale disturbances generated by the wall shear layer and their instabilities; the second is the large-scale flow with the Ekman circulation motion of fluid. The thickness of the shear layer is estimated by the expression $\delta = (\nu t)^{\frac{1}{2}}$. It is small in comparison with the cylinder radius for the characteristic time of development of the elliptical instability $t_* = \epsilon/\Omega$. The scale of circulation motion is nearly of the size of the cylinder, and hence this motion forms the initial large-scale disturbances, which may develop or not depending on the character of the system stability and the parameters of the cylinder.

For L/R regions outside the solid strips, the elliptical rotation is stable with respect to odd wavenumber n disturbances.

The character of visually observed secondary flows in region Σ_1^m corresponds to the general type of velocity field disturbances, near to the elliptical rotation around a horizontal axis in the centre of the eddy.

We have not succeeded in identifying experimentally regions of oscillation-type instability perhaps because of the condition $\sigma/\omega \ll 1$ (see also §4.3).

4. The development of instability in an ellipsoidal cavity

4.1. *General case*

Let us consider the elliptical rotation (2.1) around the z-axis in a three-axis ellipsoid

$$(x/a)^2+(y/b)^2+(z/c)^2 = 1. \tag{4.1}$$

In coordinates (2.4) it transforms into the surface

$$r = f(z'R/c) \equiv (1-(z'/l)^2)^{\frac{1}{2}}, \quad l = c/R, \quad z' = z/R. \tag{4.2}$$

System (2.9) can be investigated by expressing its solution as a series of eigenfunctions of the problem (2.12) with boundary condition (we shall omit the primes)

$$u_r r + wz/l^2 = 0 \quad (r^2+z^2/l^2 = 1). \tag{4.3}$$

The boundary condition for p_α that follows from (4.3), (2.14) is

$$\left.\begin{aligned} r\frac{\partial p_\alpha}{\partial r}+\frac{2n}{q_\alpha}p_\alpha-\frac{\lambda^2 z}{l^2}\frac{\partial p_\alpha}{\partial z} = 0 \quad (r^2+z^2/l^2 = 1), \\ \lambda^2 = (4-q_\alpha^2)/q_\alpha^2. \end{aligned}\right\} \tag{4.4}$$

Separation of variables for (2.15) and (4.4) can be obtained in the new variables (Greenspan 1968)

$$r = d[(1-\sigma^2)(1-\mu^2)]^{\frac{1}{2}}, \quad z = d\lambda\sigma\mu, \quad d^2 = (1+l^2/\lambda^2), \tag{4.5}$$

by which the region ($r \geqslant 0$, $r^2+z^2/l^2 \leqslant 1$) is mapped into a rectangle ($-\sigma_e \leqslant \sigma \leqslant \sigma_e$, $\sigma_e \leqslant \mu \leqslant 1$).

In these variables, (2.15) has the form

$$\left.\begin{aligned} (\mathrm{L}_\sigma - \mathrm{L}_\mu)\, p_\alpha = 0, \\ \mathrm{L}_\nu = (1-\nu^2)\frac{\partial^2}{\partial\nu^2}-2\nu\frac{\partial}{\partial\nu}-\frac{n^2}{1-\nu^2}, \quad \nu = \sigma, \mu. \end{aligned}\right\} \tag{4.6}$$

The solution of (4.6) should be finite at $\mu = 1$ ($r = 0$) and satisfy conditions that follow from (4.4) on the other sides of the rectangle

$$\left.\begin{aligned} (A_\sigma - A_\mu)\, p_\alpha = 0, \\ A_\nu = [1-\nu^2(1+\lambda^2/l^2)]^{-1}\left[(1-\nu^2)\,\nu\frac{\partial}{\partial\nu}-\frac{2n}{q_\alpha}\frac{1}{1+\lambda^2/l^2}\right]. \end{aligned}\right\} \tag{4.7}$$

The solution of (4.6), (4.7) has the form

$$p_\alpha = P_m^{|n|}(\sigma)\, P_m^{|n|}(\mu), \tag{4.8}$$

where $P_m^{|n|}$ are the associated Legendre polynomials; $m = |n|, |n|+1, \ldots$. The value of σ_e is defined by (4.7) as

$$\frac{1-\sigma_e^2}{\sigma_e}\frac{\mathrm{d}P_m^{|n|}}{\mathrm{d}\sigma_e}-\frac{2n}{q_\alpha}P_m^{|n|} = 0, \tag{4.9}$$

with q_α related to l and the roots of (4.9) by

$$q_\alpha^2 = 4\sigma_e^2/(l^2+(1-l^2)\,\sigma_e^2). \tag{4.10}$$

For given m and n equations (4.9), (4.10) generally define several values of σ_e and q_α, which we shall mark with the subscript j, hence $\alpha = (n, m, j)$. The eigenfunctions

$\boldsymbol{u}_\alpha, p_\alpha$ (2.14) (4.8) are polynomials of degree $m-1$ in Cartesian coordinates. Among them, there are two velocity fields for $m = 2$ and $n = 1$, which are analogous to (2.1), and eight quadratic fields. They are obtained with $m = 3$ and $n = 0, 1, 2$. For $m = 3$ and $n = 1$ there are two roots σ_e and, consequently, we obtain four quadratic fields while separating the real and imaginary parts in (2.14). Only one root σ_e corresponds to both $n = 0$ and $n = 2$, and this leads to two velocity fields in each case.

The polynomial representation is connected with another method of stability investigation in an ellipsoidal cavity that originates from the Helmholtz equations

$$\frac{\partial \boldsymbol{\Omega}}{\partial t} = \nabla \times [\boldsymbol{u}, \boldsymbol{\Omega}], \quad \boldsymbol{\Omega} = \nabla \times \boldsymbol{u}. \tag{4.11}$$

We shall write a system of basic functions that describe a non-divergent velocity field with powers of coordinates not larger than two, the normal component of which vanishes on the surface of the ellipsoid (4.1). There are three linear fields among them:

$$\left.\begin{aligned} \boldsymbol{w}_1 = bz'\boldsymbol{j} - cy'\boldsymbol{k}, \quad \boldsymbol{w}_2 = -az'\boldsymbol{i} + cx'\boldsymbol{k}, \quad \boldsymbol{w}_3 = ay'\boldsymbol{i} - bx'\boldsymbol{j}, \\ x' = x/a, \quad y' = y/b, \quad z' = z/c. \end{aligned}\right\} \tag{4.12}$$

The field $\boldsymbol{w}_3$ is proportional to the basic flow (2.1), and fields $\boldsymbol{w}_2$ and $\boldsymbol{w}_3$ correspond to the eigenfunctions $\boldsymbol{u}_\alpha$ (2.14) with $m = 2$, $n = 1$. The eight quadratic fields are taken in the form

$$\left.\begin{aligned} \boldsymbol{w}_4 &= a(y'^2 - z'^2)\boldsymbol{i} - bx'y'\boldsymbol{j} + cx'z'\boldsymbol{k}, \\ \boldsymbol{w}_5 &= a(1 - x'^2 - 2y'^2 - 2z'^2)\boldsymbol{i} + bx'y'\boldsymbol{j} + cx'z'\boldsymbol{k}, \\ \boldsymbol{w}_6 &= ax'y'\boldsymbol{i} + b(z'^2 - x'^2)\boldsymbol{j} - cy'z'\boldsymbol{k}, \\ \boldsymbol{w}_7 &= ax'y'\boldsymbol{i} + b(1 - 2x'^2 - y'^2 - 2z'^2)\boldsymbol{j} + cy'z'\boldsymbol{k}, \\ \boldsymbol{w}_8 &= -ax'z'\boldsymbol{i} + by'z'\boldsymbol{j} + c(x'^2 - y'^2)\boldsymbol{k}, \\ \boldsymbol{w}_9 &= ax'z'\boldsymbol{i} + by'z'\boldsymbol{j} + c(1 - 2x'^2 - 2y'^2 - z'^2)\boldsymbol{k}, \\ \boldsymbol{w}_{10} &= ay'z'\boldsymbol{i} - cx'y'\boldsymbol{k}, \quad \boldsymbol{w}_{11} = -bx'z'\boldsymbol{j} + cx'y'\boldsymbol{k}. \end{aligned}\right\} \tag{4.13}$$

The inhomogeneous fields $\boldsymbol{w}_5$, $\boldsymbol{w}_7$, $\boldsymbol{w}_9$ can be obtained from the toroidal fields for a sphere (Hill spherical vortex) by deforming a sphere into the given ellipsoid. The rest of the fields in (4.12), (4.13) are solenoidal functions of the form $\nabla \times g\boldsymbol{s}$, $\boldsymbol{s} = (x/a^2, y/b^2, z/c^2)$, where g is a linear or quadratic function of coordinates. Fields of this form are tangential to any ellipsoid similar to (4.1). Instead of fields $\boldsymbol{w}_5$, $\boldsymbol{w}_7$, $\boldsymbol{w}_9$ we may take inhomogeneous vector functions $\nabla \times \nabla \times (1-\rho) g\boldsymbol{s}$, $g = x, y, z$, $\rho = x^2/a^2 + y^2/b^2 + z^2/c^2$, which can also be used to obtain fields of a higher degree.

The fields (4.13) correspond to vector functions defined by (2.14) and (4.8) after separating the real and imaginary parts, so that for $m = 3$, $n = 1$ we have fields $\boldsymbol{w}_4$–$\boldsymbol{w}_7$; for $m = 3$, $n = 0$ we have $\boldsymbol{w}_9$; for $m = 3$, $n = 2$, we have $\boldsymbol{w}_8$. Linear combinations of functions with $m = 3$, $n = 0$ and $m = 3$, $n = 2$ correspond to $\boldsymbol{w}_{10}$ and $\boldsymbol{w}_{11}$.

4.2. *Wave-type instability*

Let us linearize the (4.11) with respect to $\boldsymbol{u}_0 = -\Omega \boldsymbol{w}_3$, $\boldsymbol{\Omega}_0 = \nabla \times \boldsymbol{u}_0 = \text{const.}$, $\boldsymbol{u} = \boldsymbol{u}_0 + \boldsymbol{u}'$,

$$\frac{\partial}{\partial t} \nabla \times \boldsymbol{u}' = \nabla \times [\boldsymbol{u}_0, \nabla \times \boldsymbol{u}'] + \nabla \times [\boldsymbol{u}', \boldsymbol{\Omega}_0]. \tag{4.14}$$

Since $\boldsymbol{u}_0$ is linear in the coordinates, (4.14) is homogeneous in x, y, z. Therefore its solutions may be sought in the classes of uniform functions.

Let us solve this equation in the form of superposition of basic fields (4.12), (4.13) not higher than the second power by coordinates with time-dependent coefficients. Then the right- and left-hand sides of (4.14) written in components are the sums of constant values (with respect to x, y, z) and linear functions of x, y, z. By setting the values and coefficients in the corresponding functions of x, y, z to zero we obtain the dynamic system that presents the solutions of (4.14). Thus the derived systems (4.15), (4.18), (4.23) are obtained.

For linear functions (4.12) we have the equations

$$\left.\begin{aligned} \boldsymbol{u}' &= \omega_1 \boldsymbol{w}_1 + \omega_2 \boldsymbol{w}_2, \\ (c^2+b^2)\frac{\mathrm{d}\omega_1}{\mathrm{d}t} &= (b^2-c^2)\,\Omega\omega_2, \quad (c^2+a^2)\frac{\mathrm{d}\omega_2}{\mathrm{d}t} = (c^2-a^2)\,\Omega\omega_1, \end{aligned}\right\} \tag{4.15}$$

which together with the equation for Ω,

$$(a^2+b^2)\frac{\mathrm{d}\Omega}{\mathrm{d}t} = (a^2-b^2)\,\omega_1\omega_2,$$

are the known explicit solution of (4.11) in the class of functions that are linear in the coordinates. If $\Omega = \text{const.}$, $|\omega_1/\Omega| \ll 1$, $|\omega_2/\Omega| \ll 1$, (4.15) also yields the known conditions of elliptical instability in the class of linear fields: for $a > b$ the value c must satisfy the inequality $b < c < a$, i.e. the fluid rotation around the middle axis of the ellipsoid is unstable.

In another form, this inequality is

$$2(1-\epsilon)^{\frac{1}{2}} < \frac{2c}{R} < 2(1+\epsilon)^{\frac{1}{2}}. \tag{4.16}$$

The functions $\boldsymbol{w}_1$, $\boldsymbol{w}_2$ are the fields (2.14), (4.8) with azimuthal wavenumbers $n = \pm 1$, and the axial velocity w does not change its sign along the z-axis; hence, the region of instability (4.16) corresponds to the region $\Sigma_1^1(1,1)$ of unstable elliptical rotation in a cylinder (see figure 2*a*).

The Galerkin method (3.5) for the modes (2.14), (4.8) with the wavenumbers $m = 2$, $n = \pm 1$ gives the same bounds of instability with a discrepancy in the growth rate of the order ϵ^3.

Let us consider the quadratic disturbances. The exact solution of (4.14) is the field (recall that $\boldsymbol{w}_4$–$\boldsymbol{w}_7$ correspond to $(m = 3)$, $n = \pm 1$ in connection with elliptical cylinder)

$$\boldsymbol{u}' = \sum_{i=4}^{7} \omega_i \boldsymbol{w}_i, \tag{4.17}$$

if the time-dependent parameters ω_i, $i = 4$–7, satisfy the linear system

$$\left.\begin{aligned} \frac{\mathrm{d}}{\mathrm{d}t}((2a^2+b^2)\,\omega_4 - (4a^2+b^2)\,\omega_5) &= \Omega((3b^2+2a^2)\,\omega_6 + 3b^2\omega_7), \\ \frac{\mathrm{d}}{\mathrm{d}t}((2a^2+c^2)\,\omega_4 + (4a^2+c^2)\,\omega_5) &= \Omega((4a^2-c^2)\,\omega_7 - (2a^2-c^2)\,\omega_6), \\ \frac{\mathrm{d}}{\mathrm{d}t}((2b^2+a^2)\,\omega_6 + (4b^2+a^2)\,\omega_7) &= \Omega(3a^2\omega_5 - (3a^2+2b^2)\,\omega_4), \\ \frac{\mathrm{d}}{\mathrm{d}t}((2b^2+c^2)\,\omega_6 - (4b^2+c^2)\,\omega_7) &= \Omega((2b^2-c^2)\,\omega_4 + (4b^2-c^2)\,\omega_5). \end{aligned}\right\} \tag{4.18}$$

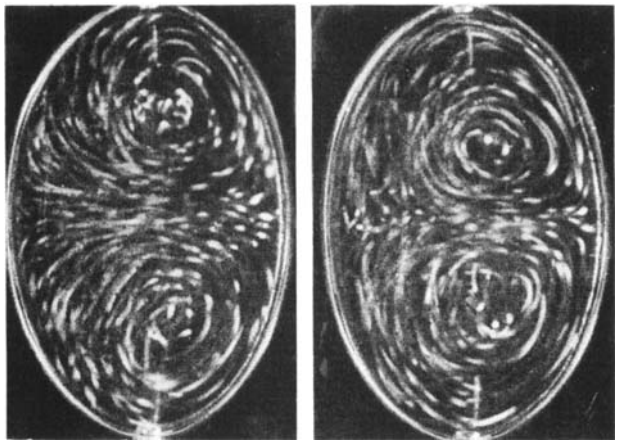

FIGURE 5. Photographs of a two-eddy flow for an ellipsoid with parameters $2c/R = 3.62$, $\epsilon = 0.38$. The interval between the frames is 0.44 s.

We arrive at the equation for the dimensionless growth rate s ($\omega_i = \exp(s\Omega t)\,\omega_i^0$):

$$As^4 + Bs^2 + C = 0, \tag{4.19}$$

$$A = [(2a^2+b^2)(4a^2+c^2)+(2a^2+c^2)(4a^2+b^2)][(2b^2+a^2)(4b^2+c^2) + (2b^2+c^2)(4b^2+a^2)],$$

$$C = [(3b^2+2a^2)(c^2-4a^2)+3b^2(c^2-2a^2)][(3a^2+2b^2)(c^2-4b^2)+3a^2(c^2-2b^2)].$$

The solution for s has the form

$$s^2 = (-B \pm (B^2-4AC)^{\frac{1}{2}})/2A. \tag{4.20}$$

Hence for instability ($s > 0$), it is sufficient that $C < 0$, since $A > 0$. That leads to the range of parameters of an ellipsoid for which the elliptical rotation is unstable under perturbations (4.17) (Gledzer & Ponomarev 1977*a*):

$$b^2\frac{9a^2+4b^2}{3a^2+b^2} < c^2 < a^2\frac{9b^2+4a^2}{3b^2+a^2}. \tag{4.21}$$

The development of unstable modes described by (4.18) gives rise to a two-eddy pattern of motion on the z-axis. The eigenvalue s is real, therefore this type of instability corresponds to the one discussed in §§3.1 and 3.2.

The other form of (4.21) is

$$[(1-\epsilon)(13+5\epsilon)/(1+\epsilon/2)]^{\frac{1}{2}} < 2c/R < [(1+\epsilon)(13-5\epsilon)/(1-\epsilon/2)]^{\frac{1}{2}}. \tag{4.22}$$

The fields $\boldsymbol{w}_4$–$\boldsymbol{w}_7$ also have the azimuthal wavenumbers $n = \pm 1$ with the axial velocity w changing sign once along the z-axis; hence, this region of instability is qualitatively the same as the region $\Sigma_1^2(1, -1)$ of unstable rotation in the elliptical cylinder.

In figure 2(*a*) the unstable regions (4.16), (4.22) in coordinates $(2c/R, \epsilon)$ are denoted by I and II, respectively. The parameters of ellipsoids for which the experiments (Gledzer *et al.* 1974; Gledzer & Ponomarev 1977*a*, *b*) were performed are marked by stars. Rotation around the largest axis is stable for ellipsoids with $2c/R = 2.54$, $\epsilon = 0.17$ and unstable for $2c/R = 3.62$, $\epsilon = 0.38$ and $2c/R = 3.06$, $\epsilon = 0.50$. Some experiments were also performed by Roesner & Schmieg (1980), who confirmed

the instability for ellipsoid $2c/R = 3.06$, $\epsilon = 0.5$ and observed the stability for ellipsoid $2c/R = 2.86$, $\epsilon = 0.3$. A picture of two-eddy secondary flow in the ellipsoid $2c/R = 3.62$, $\epsilon = 0.38$ is shown in figure 5.

4.3. *Oscillation-type instability*

Another solution of (4.14) in the class of quadratic fields has the form (the fields $\boldsymbol{w}_8$–$\boldsymbol{w}_{11}$ correspond to $m = 3$, $n = 0$ and $n = \pm 2$ for elliptical cylinder)

$$\boldsymbol{u}' = \sum_{i=8}^{11} \omega_i \boldsymbol{w}_i,$$

$$\left.\begin{aligned}
&\frac{\mathrm{d}}{\mathrm{d}t}((2c^2+b^2)\omega_8+(4c^2+b^2)\omega_9) = -\Omega((2c^2+b^2)\omega_{11}+(b^2-2c^2)\omega_{10}),\\
&\frac{\mathrm{d}}{\mathrm{d}t}((2c^2+a^2)\omega_8-(4c^2+a^2)\omega_9) = \Omega((2c^2+a^2)\omega_{10}+(a^2-2c^2)\omega_{11}),\\
&\frac{\mathrm{d}}{\mathrm{d}t}((2c^2+b^2)\omega_{11}-(2c^2+a^2)\omega_{10}) = \Omega(8c^2\omega_8+2(b^2-a^2)\omega_9),\\
&\frac{\mathrm{d}}{\mathrm{d}t}(b^2\omega_{11}+a^2\omega_{10}) = 2\Omega(a^2+b^2)\omega_9.
\end{aligned}\right\} \tag{4.23}$$

From (4.23) the equation for the eigenvalue s follows,

$$As^4+Bs^2+C = 0, \tag{4.24}$$

$$A = \kappa(8c^4+3c^2b^2+3c^2a^2+a^2b^2), \quad B = 4(\kappa(8c^4+\kappa)-c^4(a^2+b^2)^2),$$

$$C = 16c^4(a^2+b^2)^2, \quad \kappa = a^2b^2+b^2c^2+c^2a^2.$$

The solution of (4.24) is

$$s^2 = (-B\pm(B^2-4AC)^{\frac{1}{2}})/2A,$$

and since $AC > 0$, the real part of one of the roots of s is positive if

$$B^2-4AC < 0.$$

In variables $\zeta = c^2/R^2$ and ϵ this inequality takes the form

$$(\tau(8\zeta^2+\tau)-4\zeta^2)^2 < 16\zeta^2\tau(8\zeta^2+4\zeta+\tau), \quad \tau = 2\zeta+1-\epsilon^2. \tag{4.25}$$

In figure 2(*a*), this region of instability is denoted by III. It may be shown as corresponding to the region $\Sigma_1^1(0,2)$ for the elliptical cylinder.

Let us consider the behaviour of eigenvalues $s(\epsilon,\zeta)$, if $\epsilon \to 0$ in the vicinity of the corner point ζ_0 of the region of instability III. For $\epsilon = 0$, the value ζ_0 satisfies the condition (4.25), hence we have the equation

$$16\zeta_0^3-4\zeta_0-1 = 0, \quad \zeta_0 \approx 0.596. \tag{4.26}$$

If $\epsilon = 0$, $\zeta = \zeta_0$ it follows that $B = 4AC$, hence $s^2 = -B/2A$. Using (4.26), we have $s^2 = -4\zeta_0/(2\zeta_0+1) \approx -1.09$, i.e. the imaginary part of the eigenvalue is not zero. So, the instability for parameters ϵ and ζ in region III (figure 2*a*) is of the oscillation type, differing from the instability described by (4.16), (4.22) (regions I and II in figure 2*a*). This type of instability is difficult to observe experimentally.

Nevertheless, some indications of this instability may be detected on noting that superposition of the fields $\boldsymbol{w}_8, \boldsymbol{w}_9, \boldsymbol{w}_{10}, \boldsymbol{w}_{11}$, which correspond to dynamical variables of the system (4.23), in the centre of ellipsoid $x = y = z = 0$ has only the vertical

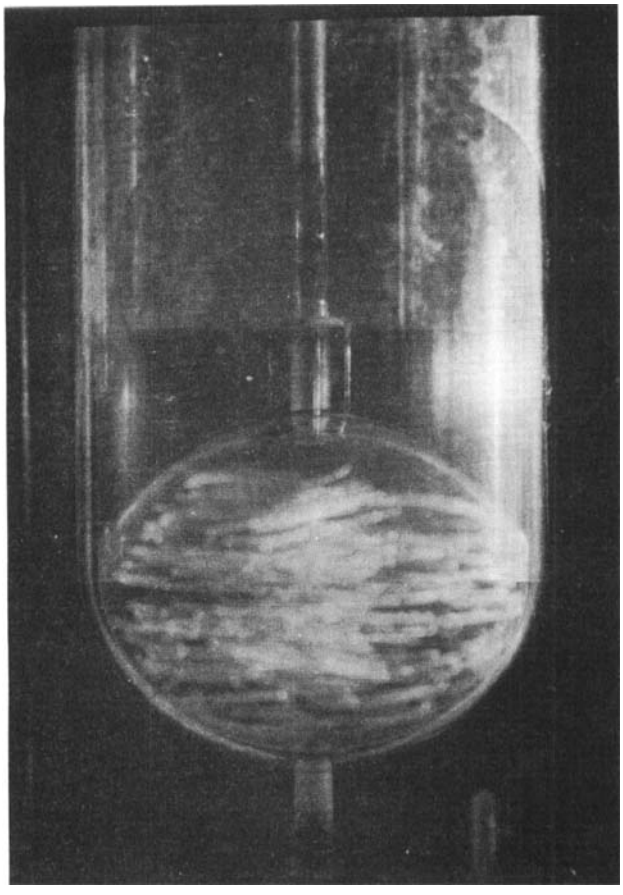

FIGURE 6. The oscillation-type instability for $2c/R = 1.6$, $\epsilon = 0.18$.

(along z-axis) component of velocity $c\boldsymbol{k}$. Therefore, the oscillations of fluid particles in the centre have to occur in the vertical direction, perpendicularly to the plane of fluid rotation. This may be observed in the experiments for an ellipsoid with $c/R = 0.8$, $\epsilon = 0.15$ (figure 6).

4.4. *Elliptical instability and the forced motion of fluid within an ellipsoid*

So far, we have considered the solutions of the linear problem of basic flow stability (2.1), where it was assumed that $\Omega = \text{const}$. For the nonlinear problem, it is necessary to close the system (2.16) by an equation for changing Ω. It is natural to use the Galerkin method retaining only a finite number of interacting modes – 'active modes' in the dynamical system obtained.

The simplest dynamical system describing the evolution of the flow in an ellipsoid must include the modes presenting the 'basic flow' and unstable disturbances. For elliptical rotation around the middle axis b, such a system has the form

$$(a^2+b^2)\dot{\Omega} = (a^2-b^2)\omega_1\omega_2 - (a^2+b^2)\lambda\Omega, \tag{4.27a}$$

$$(b^2+c^2)\dot{\omega}_1 = (b^2-c^2)\Omega\omega_2 - (b^2+c^2)\lambda\omega_1, \tag{4.27b}$$

$$(c^2+a^2)\dot{\omega}_2 = (c^2-a^2)\Omega\omega_1 + (a^2+c^2)F. \tag{4.27c}$$

Here, the term $(a^2+c^2)F$ models the force that rotates fluid around the middle axis b, and λ is the friction coefficient.

More generally, there is also a damping term $-\lambda(a^2+c^2)\,\omega_2$ in the equation for ω_2, but for large values of F the influence of this term on the steady states of (4.27) (see (4.29), (4.30)) will be negligible.

The system (4.27) may be represented in the form (we assume here that $c < b < a$)

$$\dot{\omega}_+ = p\omega_2\omega_+ - \lambda\omega_+, \quad \dot{\omega}_- = -p\omega_2\omega_- - \lambda\omega_-, \quad \dot{\omega}_2 = q(\omega_+^2 - \omega_-^2) + F, \tag{4.28}$$

$$\omega_\pm = H_1\Omega \pm H_2\omega_1, \quad H_1 = [(b^2-c^2)(a^2+b^2)]^{\frac{1}{2}}, \quad H_2 = [(a^2-b^2)(b^2+c^2)]^{\frac{1}{2}},$$

$$p = \frac{H_1H_2}{(a^2+b^2)(b^2+c^2)}, \quad q = \frac{a^2-c^2}{4(a^2+c^2)H_1H_2}.$$

The system (4.28) has two stable steady states that differ in the sign of ω_- (we suppose $F > 0$):

$$\omega_- = (F/q)^{\frac{1}{2}}, \quad \omega_+ = 0, \quad \omega_2 = -\lambda/p, \tag{4.29}$$

$$\omega_- = -(F/q)^{\frac{1}{2}}, \quad \omega_+ = 0, \quad \omega_2 = -\lambda/p. \tag{4.30}$$

It is important that if (4.28) is put into one of the states (4.29), (4.30) and then the force F is changed arbitrarily, the sign of ω_- cannot be changed during the process of motion, because the signs of ω_+ and ω_- are conserved: for regular $\omega_2(t)$ the solutions of (4.28) have the form

$$\omega_+(t) = \omega_+(0)\exp\left(\int_0^t (p\omega_2(\tau)-\lambda)\,\mathrm{d}\tau\right), \quad \omega_-(t) = \omega_-(0)\exp\left(-\int_0^t (p\omega_2(\tau)+\lambda)\,\mathrm{d}\tau\right).$$

But experiments (Obukhov, Gluckhovsky & Chernous'ko 1976) have shown that for a certain time interval from the cut-off of the force F the hydrodynamic system, for which the model (4.27) is used, transfers between the states corresponding to (4.29) and (4.30). The experiment on an ellipsoid with axis ratio 5:6:7 consisted of exciting, using a thin stirrer, elliptical rotation around the middle axis $b = 6$. This rotation rapidly lost stability (see (4.16)) and transferred to one of the stable regimes which is a superposition of elliptical rotations around the long and short axes of the ellipsoid. Then the rotation of the stirrer was stopped after a certain interval of time, when the initial motion was sufficiently intensive. On restarting the rotation of the stirrer in the same direction, the system may transfer to another steady regime or not, depending on the length of time that the external force is cut off.

Notice that the stationary states (4.29) or (4.30) are superpositions of rotations around all three axes of the ellipsoid. For a given axis ratio the rotation around the c-axis is unstable with respect to perturbations arising from the velocity fields $\boldsymbol{w}_8$–$\boldsymbol{w}_{11}$. The development of these disturbances is described by (4.23), and their action on (4.27) is given by an additional term in the right-hand side of (4.27a) that may be derived with the help of the Galerkin method used with the velocity field (4.33) below,

$$\phi = (b^2-a^2)(\omega_8(\omega_{10}+\omega_{11}) + \omega_9(\omega_{10}-\omega_{11})). \tag{4.31}$$

Equation (4.27) together with (4.23) forms a closed system for parameters Ω, ω_1, ω_2, ω_8–ω_{11}.

Note that the system (4.23), (4.27) conserves the integral (for $\lambda = 0$, $F = 0$)

$$E = (a^2+b^2)\Omega^2 + E_1 + E_2, \tag{4.32}$$

$$E_1 = (b^2+c^2)\omega_1^2 + (c^2+a^2)\omega_2^2,$$

$$E_2 = (c^2+a^2)\omega_{10}^2 - 2c^2\omega_{10}\omega_{11} + (c^2+b^2)\omega_{11}^2 + (4c^2+a^2+b^2)\omega_8^2 + 2(b^2-a^2)\omega_8\omega_9 + (8c^2+a^2+b^2)\omega_9^2,$$

which is the kinetic energy corresponding to the velocity field

$$\boldsymbol{u} = \boldsymbol{u}_0 + \omega_1 \boldsymbol{w}_1 + \omega_3 \boldsymbol{w}_3 + \boldsymbol{u}', \quad \boldsymbol{u}' = \sum_{i+4}^{11} \omega_i \boldsymbol{w}_i, \quad E = \tfrac{1}{2}\int \boldsymbol{u}^2 \, \mathrm{d}\boldsymbol{r}. \tag{4.33}$$

The conservation of the E integral (4.32) in (4.23), (4.27) in the single way gives the type of the additional term which needs to be introduced into (4.27a). So instead of the Galerkin method discussed above we may use the conservation of the energy integral E in the Galerkin approximations and system of the type of (4.23).

The equations described above were used for modelling the transitions from one steady state of the hydrodynamical system to another.

The form of the dissipation terms is defined by the experimental evidence that the relative values of Ω, ω_1, ω_2 are not affected by the value of external force F (see Obukhov *et al.* 1976), which leads to a quadratic friction $\lambda = \alpha E_1^{\frac{1}{2}}$ (α = const.). Equations (4.23) also contain dissipative terms that can be obtained by replacing the operator $\mathrm{d}/\mathrm{d}t$ by $(\mathrm{d}/\mathrm{d}t + \beta E_2^{\frac{1}{2}})$, where β = const.

As was established in §4.3 for conditions of instability (4.25), the eigenvalues $s\Omega$ have the form $(s_r \pm \mathrm{i}s_i)\,\Omega$ and $(-s_r \pm \mathrm{i}s_i)\,\Omega$, $s_r > 0$, $s_i > 0$. Converting to the basis of the corresponding eigenvectors $\boldsymbol{e}$, $\boldsymbol{e}^*$, $\boldsymbol{f}$, $\boldsymbol{f}^*$, (4.23) with damping terms introduced may be represented in the form

$$\boldsymbol{u}' = C(t)\,\boldsymbol{e} + C^*(t)\,\boldsymbol{e}^* + D(t)\boldsymbol{f} + D^*(t)\boldsymbol{f}^*, \tag{4.34}$$

$$\dot{C} = (s_r + \mathrm{i}s_i)\,\Omega C - \beta E_2^{\frac{1}{2}} C, \quad \dot{D} = (-s_r + \mathrm{i}s_i)\,\Omega D - \beta E_2^{\frac{1}{2}} D, \tag{4.35}$$

where the new variables C, D are used instead of ω_i, i = 8–11, in the quadratic form E_2, (4.32), $E_2 = E_2(C, C^*, D, D^*)$.

Now one can describe the behaviour of the system (4.28), (4.35) in the following manner. If sufficiently small initial perturbations ω_i exist, then the force F drives the system to one of the states (4.29) or (4.30), where $\lambda = aE_1^{\frac{1}{2}}$ is defined by constant values of ω_1, ω_2. So ω_2 in (4.29), (4.30) is modified as follows:

$$\omega_2 = \frac{\alpha}{2H_2} \frac{((a^2+b^2)F)^{\frac{1}{2}}}{(q(p^2 - a^2(a^2+c^2))^{\frac{1}{2}}}. \tag{4.36}$$

These solutions are unstable, and modes C and D (depending on the sign of $s_r\Omega$) are growing from small initial values. Assume $\Omega > 0$ (Ω = const. the case $\Omega < 0$ is considered analogously) that corresponds to (4.29), (4.36). Then $|D| \to 0$, and behaviour of C, C^* is described by equations

$$\left.\begin{aligned} C = A(t)\exp(\mathrm{i}s_i\Omega t), \quad \dot{A} = s_r\Omega A - \beta|A|E_2^{\frac{1}{2}}A, \\ E_2 = E_2[\exp(\mathrm{i}s_i\Omega t), \quad \exp(-\mathrm{i}s_i\Omega t), 0, 0]. \end{aligned}\right\} \tag{4.37}$$

As estimated above, $s_i \approx 1$, $s_r \ll s_i$. Hence, averaging (4.37) with respect to time yields the Landau equation

$$\dot{A} = s_r\Omega A - \beta e_0 |A| A, \tag{4.38}$$

where $e_0 = \langle E_2^{\frac{1}{2}} \rangle$ = const. > 0 is defined by the geometry of the ellipsoid. This equation describes the development of disturbances $\boldsymbol{u}'$ in the vicinity of a steady state (4.29), (4.36) and may be considered as an approximation for slowly changing functions of time $\Omega(t)$, $\omega_1(t)$, $\omega_2(t)$, $A(t)$.

The growth of disturbance $|A(t)|$ continues up to the value

$$|A|_c = \frac{s_r}{\beta e_0}\Omega;$$

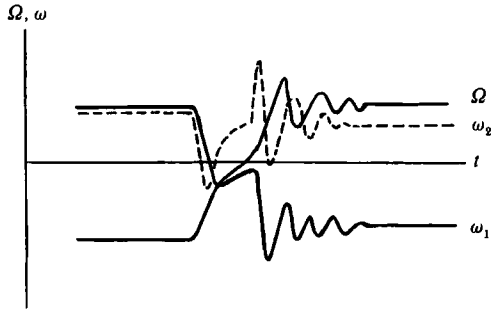

FIGURE 7. The transition between the regimes (4.29) and (4.30) in the dynamical system (4.27), (4.23) for parameters Ω, ω_1, ω_2, ω_8–ω_{11}.

hence using (4.34), (4.36) and appropriate averaging gives the approximate expression for ϕ (4.31):

$$\phi \approx (b^2-a^2)\,\phi_0\,|A|_c^2 = (b^2-a^2)\frac{s_r^2}{\beta_2}\phi'\Omega^2, \quad \phi' = \frac{\phi_0}{e_0^2},$$

and $\phi_0 = \text{const.}$ is also defined by the semiaxes of the ellipsoid.

Now (4.27) for Ω is modified in the following:

$$(a^2+b^2)\,\dot{\Omega} = (a^2-b^2)\,\omega_1\,\omega_2 - (a^2+b^2)\,aE_1^{\frac{1}{2}}\Omega + (b^2-a^2)\,\phi'\frac{s_r^2}{\beta^2}\Omega^2. \tag{4.39}$$

Hence, the influence of the last term in (4.39) may be significant if the ratio s_r^2/β^2 is large enough.

Indeed, for low values of β (for concrete numerical calculations using $F = 1$, $\alpha = 0.05$, $\beta = 0.01$) the transition between (4.29) and (4.30) occurs even for constant value of force F.

Above some value of β this transition no longer occurs for a constantly acting force F, but a transition at the removal and subsequent re-establishment of the force takes place. The results of corresponding numerical calculations are presented in figure 7. They show the possibility of transitions between the steady regimes owing to exciting the modes ω_8–ω_{11} and their action on the variables Ω, ω_1, ω_2.

In fact, in the system discussed, an indirect method of detecting the oscillation-type instability is realized. As mentioned above, the direct detecting of this instability is difficult because the growth rate to oscillations of frequency ratio s_r/s_i is small.

5. Other applications

5.1. *The influence of the Coriolis force field on the elliptical rotation*

5.1.1 *Elliptical cylinder*

In a coordinate system bound to a vessel rotating at a constant angular velocity Ω_0, (2.9a) takes the form

$$\boldsymbol{M}\left(\frac{\partial \boldsymbol{u}}{\partial t} + \boldsymbol{H}\boldsymbol{u}\right) + 2f_\epsilon\,\boldsymbol{\Lambda}\boldsymbol{u} = -\nabla p, \quad f_\epsilon = f(1-\epsilon^2)^{\frac{1}{2}}, \quad f = \Omega_0/\Omega. \tag{5.1}$$

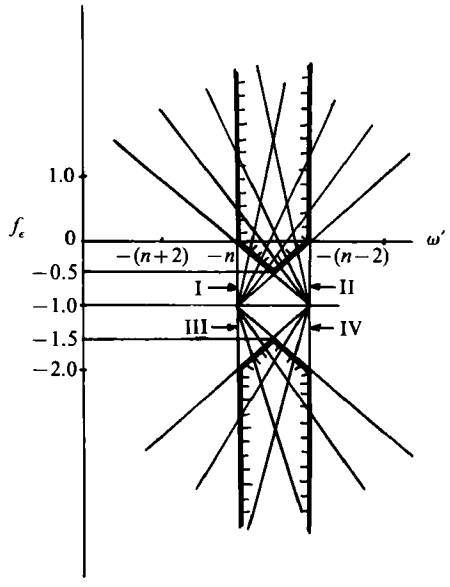

FIGURE 8. Relative positions of the spectral regions ω_α for wavenumbers n and $n-2$ in the (ω', f_ϵ)-plane.

The term $2f_\epsilon \boldsymbol{\Lambda u}$ in (5.1) does not influence the form of the eigenfunctions of the problem (2.12), but changes the eigenvalues in (2.14) in a manner determined by the frequency shift on conversion to the rotating reference frame:

$$\omega'_\alpha = (1+f_\epsilon)\, q_\alpha - n, \quad |q_\alpha| \leqslant 2, \tag{5.2}$$

where the combination $(1+f_\epsilon)$ arises from the terms $2\boldsymbol{l}\boldsymbol{\Lambda u} + 2f_\epsilon \boldsymbol{\Lambda u} = 2(1+f_\epsilon)\boldsymbol{\Lambda u}$ of equations (2.9), (5.1).

Hence, for $\epsilon \neq 0$ we shall seek a solution of (5.1) in the form of the power series (2.11), where ω_α are changed to ω'_α from (5.2). As in the case $f = 0$, the instability is possible only for degenerate or adjacent eigenvalues for wavenumbers n and $n \pm 2$. If eigenvalues coincide, $\omega'_{nl} = \omega'_{n-2,l'} = \omega'_*$, we have

$$\left.\begin{aligned} s - \omega'_* &= \pm\epsilon(1+f_\epsilon)\frac{|V_{n,l;n-2,l'}|}{N_{nl}N_{n-2,l'}}(q_{nl}q_{n-2,l'})^{\frac{1}{2}}, \\ q_{n-2,l'} &= q_{nl} - 2/(1+f_\epsilon), \end{aligned}\right\} \tag{5.3}$$

valid for fixed parameter L/R as in the case (2.18) (see also Vladimirov, Tarasov & Ribak 1983*b*).

The system (5.1) has growing solutions if

$$q_{nl}\, q_{n-2,l'} < 0. \tag{5.4}$$

Figure 8 shows the relative positions of the spectral regions ω'_α for wavenumbers n and $n-2$ in the plane $(\omega'_\alpha, f_\epsilon)$. The regions in which inequality (5.4) is satisfied are delineated in the figure. They are formed by intersections of sectors I and II, III and IV, which are bounded by the half-lines

$$f_\epsilon = \frac{\omega'+n-2}{q_{n-2}} - 1, \quad -2 \leqslant q_{n-2} < 0, \quad f_\epsilon = \frac{\omega'+n}{q_n} - 1, \quad 0 < q_n \leqslant 2,$$

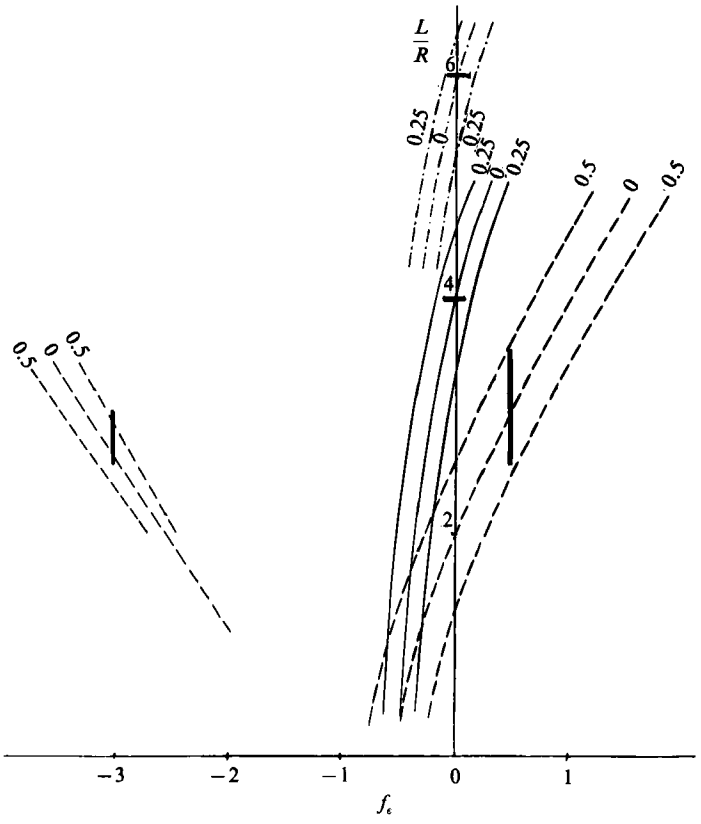

FIGURE 9. The instability regions for a flow in an elliptical cylinder in the $(L/R, f_\epsilon)$-plane. Right-hand branches: ----, $m = 1$, $n = 1$; ——, $m = 2$, $n = 1$; -·-·- $m = 3$, $n = 1$. Left-hand branches: $m = 1$, $n = 1$.

$$f_\epsilon = \frac{\omega' + n - 2}{q_{n-2}} - 1, \quad 0 < q_{n-2} \leqslant 0, \quad f_\epsilon = \frac{\omega' + n}{q_n} - 1, \quad -2 < q_n < 0,$$

respectively.

For $f = 0$, coincidence of the eigenvalues automatically guarantees satisfaction of inequality (5.4).

The results of elliptical rotation stability analysis in the Coriolis force field corresponding to the disturbances Σ_1^m are presented in figure 9 for parameters $\{f_\epsilon, L/R\}$ and fixed values of ϵ. The regions of instability reveal the same characteristics as those of Craik (1989) for unbounded rotation: there is the stable range $-\frac{3}{2} < f_\epsilon < -\frac{1}{2}$ for $\epsilon \to 0$; the unstable regions for $f_\epsilon > -1$ are broader than the region for $f_\epsilon < -1$; and the last region is narrowed at $L/R \to 0$. Figure 9 shows that the Coriolis force may both change the type of the unstable disturbances and stabilize or destabilize the elliptical rotation. These processes were illustrated by the experiments of Boubnov (1978) in an elliptical cylinder with $\epsilon = 0.18$ and $L/R = 4$ and 6, where secondary flows with 2 to 4 eddies were formed. The results of these experiments are presented in figure 10.

The experimental results for $L/R = 4$ are in good accordance with the theoretical curves on figure 9. The thick horizontal line at $L/R = 4$ gives the instability interval of f_ϵ. With $f_\epsilon = 0.1$, $L/R = 4$ we obtain stability in accordance with figure 10(f). For

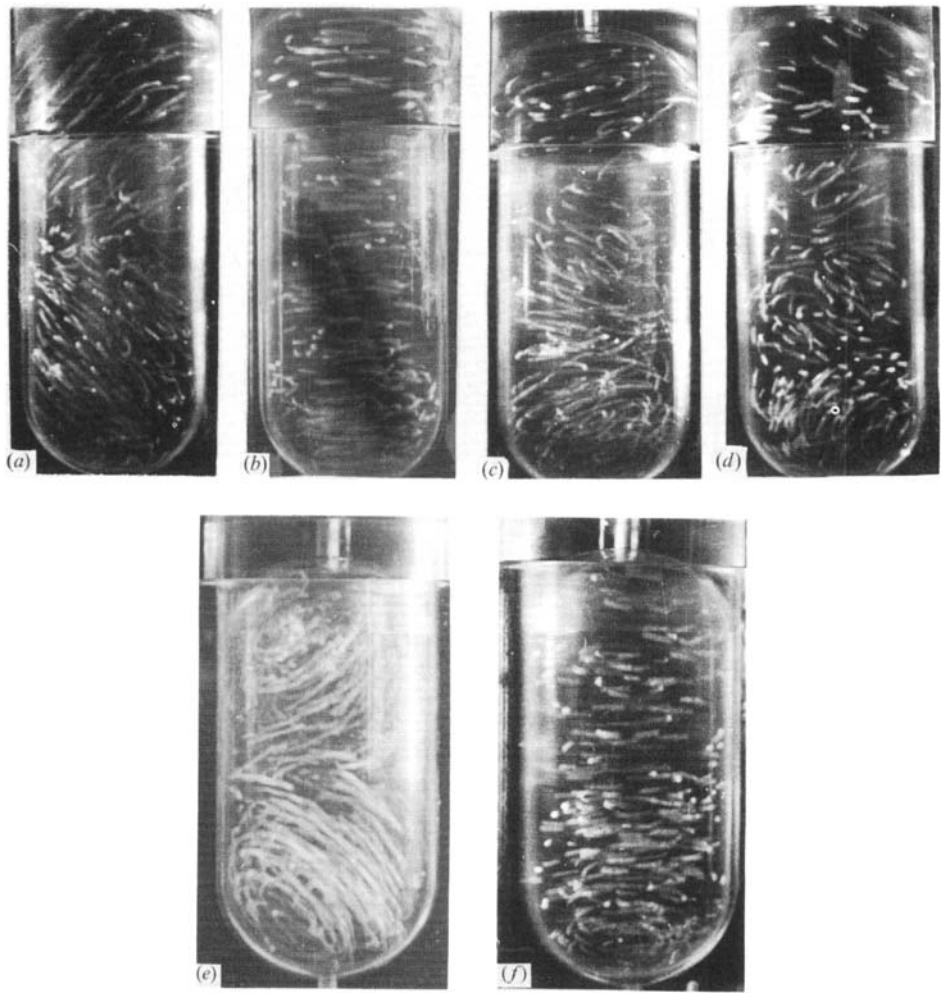

FIGURE 10. Photographs of the change in the nature of the unstable disturbances for $L/R = 6$: (a) $f = 0.1$, (b) $f = 0$, (c) $f = -0.06$, (d) $f = -0.12$; for $L/R = 4$: (e) $f = 0$, (f) $f = 0.1$.

$L/R = 6$ however the coincidence occurs only when $f_\epsilon = -0.06$ (figure 10c): this difference between theory and experiments is connected with the larger values L/R for which instability is experimentally observed than theoretically predicted values mentioned in §3.2. The validity of this two-term approximation was verified by including the additional terms in (2.11), as in §3.1. This gave a high enough accuracy for the regions of instability connected with the interaction of the equal-scale modes at $\epsilon < 0.5$ and $|f_\epsilon| < 1$.

For comparison, the results of calculations of instability intervals using (3.4), (3.11) from Craik (1989) are marked on figure 9 by thick vertical lines for $f_\epsilon = -3$ and 0.5. The ratio of the vertical and horizontal scales of disturbances is connected with Craik's parameter α_{10} by the relation $k/h = \alpha_{10}/(1-\alpha_{10}^2)^{\frac{1}{2}}$, and the value of h is chosen as for the corresponding area on figure 2(b). In spite of these planar disturbances not being compatible with the wall boundary condition, a good coincidence of the results obtained by the two approaches is notable for $f_\epsilon > 0$, although some deviations for $f_\epsilon < -1$ and considerably large ϵ are present.

5.1.2. *Ellipsoidal cavity*

The rotation of the ellipsoid as a whole, with angular velocity Ω_0 around the z-axis, yields additional terms on the right-hand sides of (4.18): $2\Omega_0 ab(\omega_6-\omega_7)$, $-4\Omega_0 ab(\omega_6-2\omega_7)$, $-2\Omega_0 ab(\omega_4+\omega_5)$, $4\Omega_0 ab(\omega_4+2\omega_5)$, respectively. Therefore B and C in the characteristic equations (4.19) are now functions of the parameter $f=\Omega_0/\Omega$:

$$C(f) = [(2a^2-c^2+2\chi)(3b^2-\chi)-(3b^2+2a^2+\chi)(c^2-4a^2-4\chi)] \times[(2b^2-c^2+2\chi)(3a^2-\chi)-(3a^2+2b^2+\chi)(c^2-4b^2-4\chi)], \quad \chi=2fab. \tag{5.5}$$

Instability occurs when parameters a, b, c satisfy the condition $C<0$, and (5.5) yields the regions of instability in the $(c/R, \epsilon, f_\epsilon)$-space given by

$$\left.\begin{aligned} l_-(\epsilon,f_\epsilon) < \frac{c}{R} < l_+(\epsilon,f_\epsilon), \\ l_\pm(\epsilon,f_\epsilon) = [(f_\epsilon+\tfrac{1}{2}(1\pm\epsilon))(f_\epsilon+\tfrac{1}{2}(13\mp 5\epsilon))/(1\mp\tfrac{1}{2}\epsilon)]^{\frac{1}{2}}. \end{aligned}\right\} \tag{5.6}$$

The projections of surfaces $l_\pm(\epsilon,f_\epsilon)$ on the $(c/R,f_\epsilon)$-plane are shown in figure 11 as solid lines. The values of ϵ are indicated near the curves. The two vertical lines joining the curves with equal values of ϵ correspond to the range of c/R in which the rotation is unstable at given ϵ and f_ϵ. Correspondingly, the horizontal lines define the instability range of f_ϵ for fixed c/R and ϵ.

It follows from (5.6) and figure 11 that the instability in a fixed ellipsoid (ϵ = const., c/R = const.) occurs for two regions of changing the angular velocity rotation of the system as a whole. (In figure 11 the left bound of the instability region for $\epsilon=0.6$ is placed at $f_\epsilon<-9$).

Also, the two-eddy instability is possible for rotation of fluid around any axis of the ellipsoid. Thus, it is necessary to choose the appropriate parameter f_ϵ.

The dashed lines in figure 11 show the one-eddy instability regions for an ellipsoid rotating as a whole, which may be calculated with the terms $2\Omega_0 ab\omega_2$ and $-2\Omega_0 ab\omega_1$ inserted in (4.15), which are valid for fields linear in coordinates. Therefore, the instability is possible if

$$l_-(\epsilon,f_\epsilon) < c/R < l_+(\epsilon,f_\epsilon), \quad l_\pm(\epsilon) = (1\pm\epsilon+2f_\epsilon)^{\frac{1}{2}}. \tag{5.7}$$

These curves are shown in figure 11.

The stars in figure 11 indicate the limit of the two-eddy instability for the ellipsoid with $c/R=1.27$, $\epsilon=0.18$ investigated experimentally by Boubnov (1978). For $f=0$ the rotation in this ellipsoid was stable.

More detailed analysis of (4.19) indicates that there are no other instability regions for disturbances $\boldsymbol{w}_4$–$\boldsymbol{w}_7$.

It is interesting that the Coriolis force field cannot change the type of instability under consideration, i.e. $B^2-4AC>0$ in (4.20) for any f.

The modification of (4.23)–(4.25) by Coriolis field terms may be considered analogously. In this case, we have the additional terms $-2fab\omega_{10}$, $2fab\omega_{11}$, $-4fab\omega_8$, $4fab\omega_9$ on the right-hand sides of (4.23). Therefore $C=C(f)$ in (4.24) must be equal to

$$C(f) = 4[2c^2(a^2+b^2)+f(4c^2-a^2-b^2)-2f^2]^2 \geqslant 0.$$

This means that the oscillation-type instability based on fields $\boldsymbol{w}_8$–$\boldsymbol{w}_{11}$ for any f also cannot be transformed into a wave-type instability with $C<0$. Thus we have shown that the types of instability cannot be transformed one into another by means of changing the coriolis parameter in the barotropic flows considered.

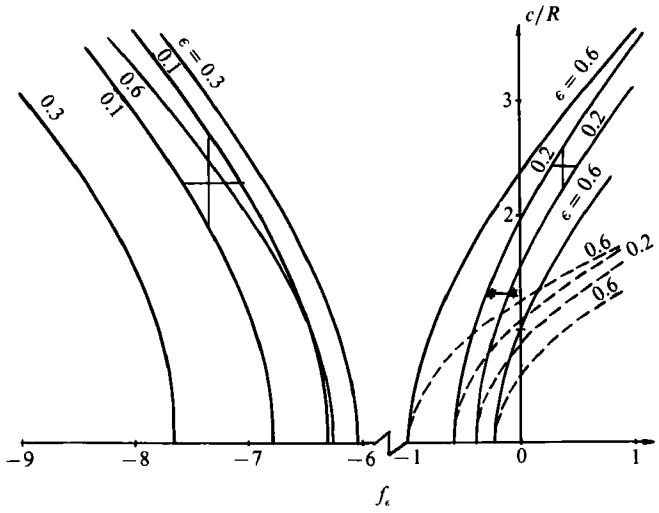

FIGURE 11. The instability regions for flow in an ellipsoid in the $(c/R, f_\epsilon)$-plane.

5.2. *The influence of the elliptical rotation on the stability of a non-uniform fluid*

Let us consider the stability of the velocity field (2.1) for the density-stratified flow equations in the Boussinesq approximation for unbounded fluid. This problem was formulated by Craik (1989). Taking the gravity acceleration $\boldsymbol{g}$ to be directed opposite to the z-axis let us present the temperature and pressure field in the form

$$T = \gamma z + T', \quad p = p_0 + p', \quad p_0 = \tfrac{1}{2}\rho[\beta g\gamma z^2 + \Omega^2(x^2+y^2)], \quad \beta = 1/T_0.$$

Using these variables and variables (2.4) and the change $T'/R \to T$, $p'/\Omega R^4 \to p$ we have the following equations instead of (2.6):

$$\mathrm{D}w = -\frac{\partial p}{\partial z} + \frac{\beta g}{\Omega} T, \quad \mathrm{D}T + w\frac{\gamma}{\Omega} = 0. \tag{5.8}$$

Eliminating T from (5.8) gives

$$(\mathrm{D}^2+\eta)\, w = -\mathrm{D}\frac{\partial p}{\partial z}, \quad \eta = \frac{\beta g\gamma}{\Omega^2}, \tag{5.9}$$

where for $\gamma > 0$, $N = (\beta g\gamma)^{\frac{1}{2}}$ is the Brunt–Väisälä frequency, $\eta = \text{const}$.

Eliminating u and v from (2.5) by virtue of the continuity equation and using (5.9) yields

$$(\mathrm{D}^2+\eta)\left[\mathrm{D}\left(\frac{1}{1+\epsilon}\frac{\partial^2}{\partial x^2} + \frac{1}{1-\epsilon}\frac{\partial^2}{\partial y^2}\right) + \frac{4\epsilon}{1-\epsilon^2}\frac{\partial^2}{\partial x\,\partial y}\right] p + \mathrm{D}(\mathrm{D}^2+4)\frac{\partial^2 p}{\partial z^2} = 0. \tag{5.10}$$

This equation is the generalization of (2.7) for non-uniform fluid and may be reduced to (2.7) by setting $\eta = 0$, $\mathrm{D}w = -\partial p/\partial z$.

In cylindrical coordinates, we seek a solution of (5.10) in the form

$$\left.\begin{aligned} p &= \mathrm{Re}\left[\exp(ikz)\sum_{-\infty}^{\infty} p_n(r,t)\exp(-in\varphi)\right], \\ (\mathrm{D}_n^2+\eta)\Big[\mathrm{D}_n\Big(\frac{\partial^2}{\partial r^2} &+ \frac{1}{r}\frac{\partial}{\partial r} - \frac{n^2}{r^2}\Big)p_n - \frac{\epsilon}{2}\left(\mathrm{D}_{n-2}G_+ p_{n+2}\right. \\ &\left. + \mathrm{D}_{n+2}G_- p_{n-2}\right)\Big] = k_\epsilon^2\,\mathrm{D}_n(\mathrm{D}_n^2+4)\,p_n, \\ G_\pm &= \Big(\frac{\partial}{\partial r} \pm \frac{n\pm 1}{r}\Big)\Big(\frac{\partial}{\partial r} \pm \frac{n\pm 2}{r}\Big), \quad \mathrm{D}_n = \frac{\partial}{\partial t} - in, \quad k_\epsilon^2 = k^2(1-\epsilon^2). \end{aligned}\right\} \tag{5.11}$$

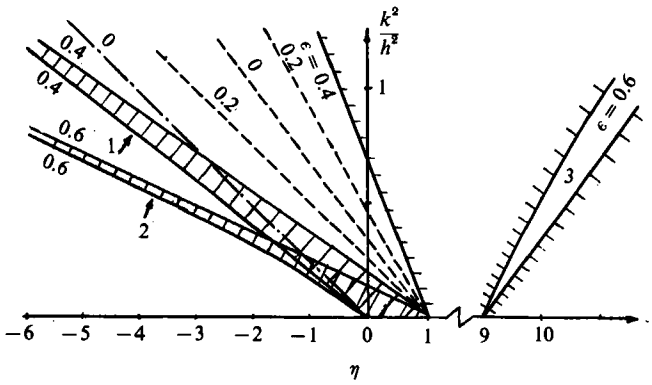

FIGURE 12. The instability regions for unbounded stratified flow in the $(k^2/h^2, \eta)$-plane: 1, the region of stability for $\epsilon = 0.4$; 2, the region of stability for $\epsilon = 0.6$; 3, the region of instability for $\epsilon = 0.6$.

Its solution is

$$p_n = \exp(int)\, J_n(hr)\, P(t), \tag{5.12}$$

$$\left(\frac{d^2}{dt^2}+\eta\right)\left[(1+\epsilon\cos 2t)\frac{dP}{dt}-4\epsilon P\sin 2t\right]+\frac{k_\epsilon^2}{h^2}\left(\frac{d^2}{dt^2}+4\right)\frac{dP}{dt}=0. \tag{5.13}$$

It is easy to show that for $\beta g\gamma = 0$ the substitution $P = \partial A/\partial t$ reduces (5.13) to the equation of Ince type described by Waleffe (1990) for uniform unbounded elliptical flow.

For $\epsilon = 0$ equation (5.13) gives the well known conditions of stability of circular rotation of non-uniform fluid: stability at $\beta g\gamma > -4\Omega^2k^2/h^2$ and instability at $\beta g\gamma < -4\Omega^2k^2/h^2$. Here the usual condition of stability $\gamma > 0$ (temperature increasing or density decreasing) without rotation for the rotation case is replaced by a weaker one.

Certainly (5.13) may be obtained from (5.10) by a substitution similar to (2.8), since for $p(r,t)$ an equation equivalent to (3.10) for $w(r,t)$ can be written.

To solve (5.13), let us present it in the form

$$P = \exp(ist)\sum_n C_n \exp(-int). \tag{5.14}$$

Substituting (5.14) in (5.13) gives the following equations for the C_n:

$$(s-n)\left[\eta+4q_\epsilon^2-(1+q_\epsilon^2)(s-n)^2\right]C_n+\frac{\epsilon}{2}\left[\eta-(s-n)^2\right]\left[(s-n+2)\,C_{n+2}\right.$$

$$\left.+(s-n-2)\,C_{n-2}\right]=0, \quad q_\epsilon^2=\frac{k_\epsilon^2}{h^2}.$$

For small ϵ this system can be truncated to keep only C_1 and C_{-1}, giving the instability boundary as

$$1-\frac{3k^2}{h^2}\left(1+\frac{3\epsilon}{2}\right)<\eta<1-\frac{3k^2}{h^2}\left(1-\frac{3\epsilon}{2}\right). \tag{5.15}$$

For arbitrary values of ϵ the numerically calculated region of instability is shown

in figure 12 within the areas enclosed by lines $\epsilon = \text{const.}$ ($\epsilon = 0.2, 0.4, 0.6$) originating from the point $\beta g\gamma/\Omega^2 = 1$, $k^2/h^2 = 0$.

As was noted for $\beta g\gamma/\Omega^2 < -4k^2/h^2$ at $\epsilon = 0$, the rotation is unstable (the region to the left of the dashed line $\epsilon = 0$ starting from the origin of the coordinates). Numerical calculations show that an interval of k^2/h^2 exist for fixed ϵ and $\beta g\gamma/\Omega^2$, for which the elliptical rotation is stable. It is located within the instability region for $\epsilon = 0$. Here, equation (5.13) demonstrates behaviour analogous to a stable pendulum with a vibrating point of suspension. The corresponding regions of k^2/h^2 and $\beta g\gamma/\Omega^2$ are located between lines $\epsilon = \text{const.}$ in the left part of figure 12 (in figure 12 $\epsilon = 0.4$, 0.6). These regions become narrower with increasing k^2/h^2 and $|\eta|$.

Another instability region of (5.13) originates from the point $\eta = 9$. The corresponding region of instability of (5.13) is shown in figure 12 for $\epsilon = 0.6$. Note, that this region turns out to be narrower than the main region of instability (5.15).

6. Conclusions

Attention in this paper was devoted mainly to the types of elliptical instability in vessels of elliptical section. The wave and oscillation types of instability were considered using two modifications of the Galerkin method. The first is based on the system of functions which represent the inertial waves in fluid rotating as a solid body. It can be applied to volumes of arbitrary elliptical section. A representation of the velocity field as polynomials in the coordinates was used for flows in the three-axis ellipsoid, which leads to exact solutions of the linear stability problem.

The wave-type instability is a system of spatial waves with monotone amplitude growth. The oscillation-type instability is determined by perturbations that oscillate with frequencies close to the angular frequency of the basic elliptical rotation, which makes it difficult to observe in experiments.

The regions of instability for an elliptical cylinder and a three-axis ellipsoid coincide with experimentally defined regions for disturbances with a small number of eddies (see figure 2*a*).

The influence of the Coriolis force field on the stability of elliptical rotation is discussed. It is characterized by the ratio of general rotation angular velocity to the value of the elliptical rotation of fluid $f = \Omega_0/\Omega$. It is shown that for small values of the ellipticity parameter ϵ, the elliptical rotation is stable in the linear approximation for $-\frac{3}{2} < f < -\frac{1}{2}$. The change of parameter f may stabilize or destabilize the elliptical rotation and change the unstable modes for a given vessel but not the type of instability.

A method connected with the w-equation (2.7) (or for pressure p (5.10)) may be applied to investigate the elliptical instability of unbounded stratified flows. The regions of instability that were absent for circular rotation of fluid are described in the plane of parameters $(k^2/h^2, \eta)$, where k/h and $\eta^{\frac{1}{2}} = N/\Omega_0$ are the non-dimensional wavenumber and Brunt–Väisälä frequency (figure 12). The phenomenon of stabilization of elliptical rotation was also found with respect to the unstable perturbations that existed for circular flow with unstable temperature stratification.

Professor A. M. Obukhov discussed the ideas of this paper in summer 1989. Also the authors would like to thank Dr B. M. Boubnov for providing the photographs in figure 10 and Professor F. V. Dolzhansky for helpful discussions.

REFERENCES

BAYLY, B. J. 1986 Three-dimensional instability of elliptical flow. *Phys. Rev. Lett.* **57**, 2160–2171.

BAYLY, B. J., ORSZAG, S. A. & HERBERT, T. 1988 Instability mechanisms in shear-flow transition. *Ann. Rev. Fluid Mech.* **20**, 359–391.

BOUBNOV, B. M. 1978 Effect of Coriolis force field on the motion of a fluid inside an ellipsoidal cavity. *Izv. Atmos. Ocean. Phys.* **14**, 501–504.

CHERNOUS'KO, YU. L. 1978 An experimental study of secondary multi-eddy flows in elliptical cylinders. *Izv. Atmos. Ocean. Phys.* **14**, 151–153.

CRAIK, A. D. D. 1988 A class of exact solutions in viscous incompressible magnetohydrodynamics. *Proc. R. Soc. Lond.* A **417**, 235–244.

CRAIK, A. D. D. 1989 The stability of unbounded two- and three-dimensional flows subject to body forces: some exact solutions. *J. Fluid Mech.* **198**, 275–295.

CRAIK, A. D. D. & CRIMINALE, W. O. 1986 Evolution of wavelike disturbances in shear flows: a class of exact solutions of the Navier–Stokes equations. *Proc. R. Soc. Lond.* A **406**, 13–26.

GLEDZER, E. B., DOLZHANSKY, F. V. & OBUKHOV, A. M. 1981 *Hydrodynamic Type Systems and their Applications*. Moscow: Nauka.

GLEDZER, E. B., DOLZHANSKY, F. V., OBUKHOV, A. M. & PONOMAREV, V. M. 1975 An experimental and theoretical study of the stability of motion of a liquid in an elliptical cylinder. *Izv. Atmos. Ocean. Phys.* **11**, 617–622.

GLEDZER, E. B., MAKAROV, A. L. & PONOMAREV, V. M. 1980 Stability of elliptical fluid rotation in a Coriolis force field. *Isv. Atmos. Ocean. Phys.* **16**, 280–282.

GLEDZER, E. B., NOVIKOV, YU. V., OBUKHOV, A. M. & CHUSOV, M. A. 1974 An investigation of the stability of liquid flows in a three-axis ellipsoid. *Isv. Atmos. Ocean. Phys.* **10**, 69–71.

GLEDZER, E. B. & PONOMAREV, V. M. 1977*a* Finite-dimensional approximation of the motions of an incompressible fluid in an ellipsoid cavity. *Isv. Atmos. Ocean. Phys.* **13**, 565–569.

GLEDZER, E. B. & PONOMAREV, V. M. 1977*b* On the forced motion of fluid within an ellipsoid. *Isv. Atmos. Ocean. Phys.* **13**, 687–689.

GREENHILL, A. G. 1879 On the rotation of a liquid ellipsoid about its mean axis. *Proc. Camb. Phil. Soc.* **3**, 233–246.

GREENSPAN, H. P. 1968 *The Theory of Rotating Fluids*. Cambridge University Press.

HERBERT, T. 1983 Secondary instability of plane channel flow to subharmonic tree-dimensional disturbances. *Phys. Fluids* **26**, 871–874.

HOUGH, S. S. 1895 The oscillations of a rotating ellipsoidal shell containing fluid. *Phil. Trans. R. Soc. Lond.* A **186**, 469–506.

LANDMAN, M. J. & SAFFMAN, P. G. 1987 The three-dimensional instability of strained vortices in a viscous fluid. *Phys. Fluids* **30**, 2339–2342.

MALKUS, W. V. R. 1989 An experimental study of global instabilities due to the tidal (elliptical) distortion of a rotating elastic cylinder. *Geophys. Astrophys. Fluid Dyn.* **30**, 123–134.

MALKUS, W. V. R. & WALEFFE, F. 1991 The transition from order to disorder in elliptical flow: a direct path to shear flow turbulence. In *Advances in Turbulence 3* (ed. A. H. Johansson & P. V. Alfredson). Springer.

MCEWAN, A. D. 1970 Inertial oscillations in a rotating fluid cylinder. *J. Fluid Mech.* **40**, 603–640.

OBUKHOV, A. M. & DOLZHANSKY, F. V. 1975 On simple models for simulation of nonlinear processes in convection and turbulence. *Geophys. Fluid Dyn.* **6**, 195–209.

OBUKHOV, A. M., GLUKHOVSKY, A. B. & CHERNOUS'KO, YU. L. 1976 Reversal phenomena in the simplest fluid-dynamic systems. *Isv. Atmos. Ocean. Phys.* **12**, 693–693.

ORSZAG, S. A. & PATERA, A. T. 1983 Secondary instability of wall bounded shear flows. *J. Fluid Mech.* **128**, 347–385.

PIERREHUMBERT, R. T. 1986 Universal short-wave instability of two-dimensional eddies in an inviscid fluid. *Phys. Rev. Lett.* **57**, 2157–2159.

PIERREHUMBERT, R. T. & WIDNALL, S. E. 1982 The two- and three-dimensional instabilities of a spatially periodic shear layer. *J. Fluid Mech.* **114**, 59–82.

POINCARÉ, H. 1910 Sur la precession des corps deformables. *Bull. Astr.* **27**, 321–356.

ROBINSON, A. C. & SAFFMAN, P. G. 1984 Three-dimensional stability of an elliptical vortex in a straining field. *J. Fluid Mech.* **142**, 451–466.

ROESNER, K. G. & SCHMIEG, H. 1980 Instabilities of spin-up and spin-down flows inside of liquid-filled ellipsoids. *Proc. Colloque Pierre Curie, 1–5 Sept., 1980, Paris.*

TSAI, C.-Y. & WIDNALL, S. E. 1976 The stability of short waves on a straight vortex filament in a weak externally imposed strain field. *J. Fluid Mech.* **73**, 721–733.

VLADIMIROV, V. A. & ILYJN, K. I. 1988 Three-dimensional instability of an elliptical Kirchhoff vortex. *Mech. Zhid. i Gaza* No. 3, 40–45 (in Russian).

VLADIMIROV, V. A., RIBAK, L. YA & TARASOV, V. F. 1983*a* Experimental and theoretical investigation of the stability of a linear vortex with a deformed core. *Prikl. Mech. Tekhn. Fis.* No. 3, 61–69 (in Russian).

VLADIMIROV, V. A., TARASOV, V. P. & RIBAK, L. YA. 1983*b* On stability of elliptically deformed rotation of ideal incompressible fluid in the field of Coriolis forces. *Isv. Atmos. Ocean. Phys.* **19**, 586–594 (in Russian).

WALEFFE, F. 1990 On the three-dimensional instability of strained vortices. *Phys. Fluids* A **2**, 76–80.